

# On the geometry of quantum complexity

Roberto Auzzi<sup>a,b</sup>, Stefano Baiguera<sup>c</sup>, G. Bruno De Luca<sup>d</sup>  
Andrea Legramandi<sup>e</sup>, Giuseppe Nardelli<sup>a,f</sup> and Nicolò Zenoni<sup>a,b,g</sup>

<sup>a</sup> *Dipartimento di Matematica e Fisica, Università Cattolica del Sacro Cuore,  
Via Musei 41, 25121 Brescia, Italy*

<sup>b</sup> *INFN Sezione di Perugia, Via A. Pascoli, 06123 Perugia, Italy*

<sup>c</sup> *The Niels Bohr Institute, University of Copenhagen Blegdamsvej 17,  
DK-2100 Copenhagen Ø, Denmark*

<sup>d</sup> *Stanford Institute for Theoretical Physics, Stanford University, Stanford, CA 94306*

<sup>e</sup> *Department of Physics, Swansea University, Swansea SA2 8PP, United Kingdom*

<sup>f</sup> *TIFPA - INFN, c/o Dipartimento di Fisica, Università di Trento,  
38123 Povo (TN), Italy*

<sup>g</sup> *Instituut voor Theoretische Fysica, KU Leuven, Celestijnenlaan 200D, B-3001 Leuven,  
Belgium*

E-mails: roberto.auzzi@unicatt.it, stefano.baiguera@nbi.ku.dk,  
gbdeluca@stanford.edu, andrea.legramandi@swansea.ac.uk,  
giuseppe.nardelli@unicatt.it, nicolo.zenoni@unicatt.it

## Abstract

Computational complexity is a new quantum information concept that may play an important role in holography and in understanding the physics of the black hole interior. We consider quantum computational complexity for  $n$  qubits using Nielsen's geometrical approach. We investigate a choice of penalties which, compared to previous definitions, increases in a more progressive way with the number of qubits simultaneously entangled by a given operation. This choice turns out to be free from singularities. We also analyze the relation between operator and state complexities, framing the discussion with the language of Riemannian submersions. This provides a direct relation between geodesics and curvatures in the unitaries and the states spaces, which we also exploit to give a closed-form expression for the metric on the states in terms of the one for the operators. Finally, we study conjugate points for a large number of qubits in the unitary space and we provide a strong indication that maximal complexity scales exponentially with the number of qubits in a certain regime of the penalties space.

# Contents

<b>1</b>	<b>Introduction</b>	<b>1</b>
<b>2</b>	<b>Unitary complexity</b>	<b>4</b>
2.1	Comments on the choice of basis . . . . .	5
2.2	Connection and geodesic equation . . . . .	6
2.3	Riemann tensor . . . . .	6
2.4	Sectional curvatures . . . . .	6
2.5	Ricci tensor and curvature . . . . .	7
<b>3</b>	<b>Few qubits examples</b>	<b>8</b>
3.1	One qubit . . . . .	8
3.2	Two qubits . . . . .	10
<b>4</b>	<b>Many qubits</b>	<b>11</b>
4.1	Counting non-vanishing sectional curvatures . . . . .	11
4.2	Draconian penalties . . . . .	13
4.3	Towards a more sustainable taxation policy . . . . .	14
4.4	Progressive penalties . . . . .	15
<b>5</b>	<b>State complexity and submersions</b>	<b>17</b>
5.1	Submersions . . . . .	18
5.2	Submersions and complexity geometry . . . . .	19
5.3	Submersions and curvature . . . . .	21
5.4	Submersion for 1 qubit . . . . .	21
5.5	Qutrits . . . . .	22
5.6	Submersions and geodesics . . . . .	26
<b>6</b>	<b>Towards an exponential complexity</b>	<b>28</b>
6.1	Conjugate points and Raychaudhuri equation . . . . .	28
6.2	An application to a simple class of geodesics . . . . .	29
6.3	One qubit . . . . .	30
6.4	Draconian model . . . . .	32
6.5	Progressive model . . . . .	33
<b>7</b>	<b>Conclusions</b>	<b>35</b>
<b>A</b>	<b>Shear tensor equation</b>	<b>37</b>

## 1 Introduction

An important problem in theoretical quantum computation is to determine the best quantum circuit to implement a desired unitary transformation. In general, this might be a challenging question. Moreover, it would be nice to have better theoretical tools to prove if a quantum computation problem has or not an efficient solution. The concept of quantum computational complexity has been introduced to answer these questions. Complexity itself is defined in a rather heuristic way as the minimal number of computational gates required to build a given unitary operator with some tolerance. In order to improve the quantitative understanding, a geometrical approach to computational complexity in quantum mechanics was introduced in [1] and further studied in [2, 3, 4, 5]. The basic idea is to introduce a Riemannian metric in the space of unitary operators acting on a given number

of qubits, which quantifies how hard it is to implement a given quantum computational task. The distance induced by the metric in the space of unitary operators is used as a measure of the complexity of the quantum operation.

An additional motivation to study complexity arises from the desire of understanding the physics of the black hole interior [6, 7, 8, 9, 10]. Quantum information theory already provided us with many insights along the road to understand quantum aspects of gravity. This is especially powerful in the framework of AdS/CFT. The concept of entanglement entropy has a natural dual in terms of area of extremal surfaces [11]. Recently, such a geometric realisation of entanglement led us to a better understanding of the Page curve [12] for an evaporating black hole, see e.g. [13, 14, 15].

It is natural to conjecture that other features of holographic spacetime are encoded in other quantum information quantities, such as complexity. In the context of AdS/CFT correspondence, the growth of computational complexity was proposed as the boundary dual of the growth of the size of the Einstein-Rosen bridge connecting the left and the right sides of an eternal black hole in AdS. Two main holographic duals for complexity were proposed:

- the complexity=volume (CV) conjecture relates complexity to the volume of an extremal slice anchored to the boundary [6, 7, 8];
- the complexity=action (CA) conjecture relates complexity to the action computed in the Wheeler-DeWitt patch [16, 17].

Holographic complexity was recently studied in a large variety of settings, see e.g. [18, 19, 20, 21, 22, 23, 24, 25]. Another promising generalisation is provided by subregion complexity [26, 27, 28, 29, 30, 31, 32, 33, 34, 35, 36, 37, 38, 39]. The appropriate notion of complexity in quantum field theory, dual to these holographic quantities, is still an open problem. One of the most promising and challenging approaches is to generalise Nielsen's geometric method to quantum field theory, see e.g. [40, 41, 42, 43, 44, 45].

A conjecture about the generic time evolution of complexity has been proposed in [9]. In this picture, at early times complexity grows linearly for a period that is exponential in the number of qubits  $n$ . This initial phase is called the complexity ramp. At time  $t \propto e^n$  it reaches its maximum value and then it flattens for a very long time  $t \propto e^{e^n}$ , doubly exponential in  $n$  (this is called the complexity plateau). After this very long time, quantum recurrence can bring back the system to sub-exponential values with non-negligible probability. This picture, if confirmed, would give us interesting insights on the quantum history of black holes. For instance, white holes could be thought of as the gravity duals of a phase of decreasing complexity due to quantum recurrence.

The geometrical approach by Nielsen is an interesting direction to put the definition of complexity on firmer grounds. There is an important order zero property that complexity must satisfy in order to fit the expectations in [9]: in the limit of large number of qubits  $n$ , the maximal complexity should scale exponentially with  $n$ .

A full understanding of complexity is still an open problem already in quantum mechanics. In particular, there are many ways to define geometric computational complexity. Riemannian geometry is just a possibility. It could be that Finsler geometry is more appropriate to investigate complexity, both for quantum computer science [1] and in the holographic case [44]. Even in the more traditional paradigm of Riemannian geometry, there is a lot of ambiguity in defining complexity. Part of it comes from the choice of the penalty factors for the Hermitian generators of the unitary transformations, which implement the physical concept that some operations can be harder than others to perform in a quantum circuit. The simplest possibility would be to choose a uniform penalty factor, independent of the number of qubits entangled by the given quantum operation. However

this brings to a maximal allowed complexity which does not scale exponentially with the number of qubits [1] and so it does not match our expectations. It was suggested in [1] that Finsler metrics with uniform penalty factors or Riemannian metrics with non-uniform penalties may instead give an exponential complexity in some regions of the parameter space.

An interesting toy model for many desired features of complexity geometry was proposed in [46], considering geodesics in a compact 2-dimensional space with negative curvature. In particular, it was argued that negative curvature gives an interesting crossover between  $L^2$  norm at small distances and an effective  $L^1$  norm at large distances. This allows us to remain in the framework of Riemannian geometry, which is easier to deal with compared to Finsler geometry.

Another desirable property of complexity metric is the ergodicity of geodesics, which is important to apply thermodynamical arguments to complexity evolution [47, 48, 49]. Ergodicity in this context refers to the general idea that the trajectory of a generic state along a geodesic will eventually visit all the allowed portions of the unitary space. There are classical mathematical results (see e.g. [51]) showing that the geodesic flow on a manifold with all negative sectional curvatures is ergodic. The complexity metric with uniform penalty factors is positively curved in all the directions and does not have an ergodic geodesic flow. The introduction of non-uniform penalty factors can make some of the sectional curvatures negative [5], but not all of them. If the negative contribution dominates, we expect that the geodesic motion is still ergodic.

Let us denote with  $w$ , which we will refer to as the *weight*, the number of qubits which are simultaneously entangled by a given generator. In [5], the following choice of penalty factors was studied in detail for systems of  $n$  qubits:

$$\begin{aligned} q(w) &= 1, & w \leq 2, \\ q(w) &= q, & w > 2. \end{aligned} \tag{1.1}$$

In order to get negative scalar curvature, a penalty factor  $q$  of order  $4^n$  is needed. This brings to a singular limit where the negative scalar curvature is dominated by a few negative sectional curvatures which diverge in the large  $n$  limit. The penalty choice in (1.1) was called *draconian* in [47]. It was argued that this choice is not appropriate to reproduce black hole properties such as scrambling time and switchback effect [50].

For this reason, in [47] a less drastic choice of penalty factors was advocated. In this paper we will study a variant of this choice:

$$q(w) = \alpha^{w-1}, \tag{1.2}$$

where  $\alpha > 1$  is a constant. We will call the choice (1.2) *progressive penalties*. In order to understand complexity geometry in an analytic way, we will propose a large  $\alpha$  limit in which complexity geometry might be studied order by order in the expansion parameter  $\alpha^{-1}$ . The leading order sectional curvatures scale as  $\alpha^0$ . We find closed form for all the curvatures up to the next-to leading order  $\alpha^{-1}$ .

As recently emphasised in [52], two different but strongly related definitions of complexity can be considered for quantum systems:

- Unitary complexity quantifies how hard it is to build some unitary operators. It was physically motivated by the problem of quantum circuit computational complexity [1, 2, 3, 4, 5].
- State complexity quantifies how hard it is to build a unitary transformation which transforms the reference state to the target state [6, 7, 8, 10]. This is the most natural way to apply the notion of complexity to holography.

For  $n$  qubits, the unitary complexity metric is defined on the group manifold  $SU(2^n)$  and it is a homogeneous but not isotropic metric. In particular, homogeneity tells us that scalar quantities (such as curvature) are constant. The state complexity metric instead is defined on  $\mathbb{CP}^{2^n-1}$  and it is neither isotropic nor homogeneous. The number of dimensions is smaller than in the unitary metric, but the geometrical structure is more complicated, because this space is not homogeneous and the scalar curvature is not constant. In this paper we point out that the relation between unitary and states complexity is a particular case of Riemannian submersion [53]. For this reason, geodesics on the state space are determined by just projecting a class of geodesics on the unitary space, the horizontal ones [54]. Moreover, the curvatures in the state space can be obtained from the curvatures in the unitary space by O'Neill's formula [53].

Complexity is determined (both in unitary and state spaces) as the length of the shortest geodesic which connects two given points. Given a geodesic starting from an initial point  $P$ , there exists another point along the geodesic where it begins to fail to be the minimal one. This is called the cut point of the geodesic. The cut locus of a given point  $P$  is defined as the set of all the cut points of the geodesics starting from  $P$ . For unitaries complexity, the metric is homogeneous and then it is enough to study the cut locus at the identity. In general to find the cut locus is a complicated problem. A useful approach is to consider conjugate points which, roughly speaking, are the points of the manifold that can be joined by a continuous 1-parameter family of geodesics. From a general result in geometry, we know that a given geodesic fails to be the minimising one after its first conjugate point. The converse is not true: a geodesic may stop to be minimising well before a conjugate point is reached. In this paper we study conjugate points of complexity metric both for one and for a large number of qubits. From this analysis, we find an evidence that maximal complexity scales exponentially with  $n$  in the progressive model for large  $\alpha$ .

The paper is organised as follows. In section 2 we review some results of [5] for the complexity geometry in the unitary space for an arbitrary number of qubits and we derive a useful explicit formula for sectional curvatures. In section 3 we briefly discuss some few qubits examples. In section 4 we consider the situation of a large number of qubits  $n$ : after a brief review of the draconian case, we study the progressive choice of penalties (1.2). In section 5 we discuss state complexity and we point out the relevance of the Riemannian submersion, which relates the geometry of the states to the one of the unitaries. We also derive a closed-form expression for the state metric and we apply it to the case of one qutrit. In section 6 we study the conjugate points in the unitary space of a simple class of geodesics, given by the exponential of the generators which are eigenvalues of the penalty matrix. We conclude in section 7.

## 2 Unitary complexity

We will first review several useful results about the geometry of unitary complexity, following [5]. We will consider the spaces of unitary operators acting on a  $n$  qubits system, which is  $SU(2^n)$ . The tangent vector at a generic point  $U_0$  can be specified in terms of a traceless Hermitian generator  $H$ , which is the tangent to the curve

$$U(t) = e^{-iHt}U_0, \quad (2.1)$$

evaluated at  $t = 0$ .

For a generic curve  $U(t)$  in the space of unitaries determined by the Schrödinger equation  $\dot{U}(t) = -iH(t)U(t)$ , we can define in general a complexity norm using a suitable Riemannian metric:

$$l = \int dt \langle H(t), H(t) \rangle^{1/2}. \quad (2.2)$$

In our application, we will consider  $\langle \dots \rangle$  to be a positive-definite inner product and independent from the group point  $U$ . Such a metric can be therefore defined at the origin of the group manifold and it can be mapped to every point of the manifold using right-translations. This a metric is usually called a right-invariant metric [55, 56] and can be defined starting from a given scalar product at the origin:

$$\langle H, K \rangle = \frac{\text{Tr} [H\mathcal{G}(K)]}{2^n}. \quad (2.3)$$

Here  $\mathcal{G}$  is a positive-definite operator on the space of unitaries, i.e. a superoperator<sup>1</sup>.

## 2.1 Comments on the choice of basis

We work with the basis defined by generalised Pauli matrices  $\sigma$ , which are nothing but the tensor products of  $n$  matrices, each of which can be either a  $SU(2)$  Pauli matrix  $\sigma_i$  ( $i = 1, 2, 3$ ) or the identity  $\mathbb{1}_2$ . We define the *weight*  $w(\sigma)$  as the number of  $SU(2)$  Pauli matrices involved in the tensor product  $\sigma$ . We will consider only diagonal metrics in our basis, i.e.  $\mathcal{G}(\sigma) = q_\sigma \sigma$ , so that the inner-product (2.3) reads

$$\langle \sigma, \tau \rangle = q_\sigma \delta_{\sigma\tau}, \quad (2.4)$$

and we denote by  $q_\sigma$  the penalty factor for the generator  $\sigma$  normalized as  $\text{Tr}(\sigma^2) = 2^n$ . We call the choice  $q_\sigma = 1$  the unpenalised choice.

The generalised Pauli matrices have a useful property: if we choose two elements of the basis, they either commute or anti-commute. In the one qubit case this follows directly from the Pauli matrices algebra, and it can be easily generalised to  $n$  qubits case. In particular, let us consider the product  $\tau\mu$  of two generalized Pauli matrices, then we have

$$\mu\tau = (-1)^l \tau\mu, \quad (2.5)$$

where  $l$  is the number of the corresponding entries in the tensor products in  $\tau$  and in  $\mu$  involving different Pauli matrices.

It is useful to count the number of generalized Pauli matrices anticommuting with a given  $\sigma$ . If  $\sigma = \mathbb{1}$ , trivially there are no operators anticommuting with it. If  $\sigma \neq \mathbb{1}$ , a generalized Pauli matrix  $\rho$  anticommutes with it under the condition that there is an odd number  $l$  of corresponding entries in the tensor products in  $\sigma$  and  $\rho$  involving different Pauli matrices. Let us suppose that  $\sigma$  has weight  $w$  (its tensor product contains  $w$  Pauli matrices). Then, we necessarily have  $0 \leq l \leq w$ . Among the  $n$  entries of the tensor product in  $\rho$ , the  $n - w$  entries in correspondence with the identity  $\mathbb{1}_2$  in  $\sigma$  can arbitrarily be any matrix in the basis ( $\mathbb{1}_2, \sigma_i$ ) indifferently. Thus we have  $4^{n-w}$  choices for such entries. For the remaining  $w$  entries of  $\rho$ , we have  $\binom{w}{l}$  choices for the  $l$  positions of the unequal Pauli matrices. Once this is fixed, there is a further  $2^w$  degeneracy of choices. Summarizing, the number of generalized Pauli matrices  $\rho$  anticommuting with  $\sigma$  is

$$4^{n-w} \sum_{l \text{ odd}=1}^w \binom{w}{l} 2^w = \frac{4^n}{2^w} \sum_{l'=0}^{\lfloor \frac{w-1}{2} \rfloor} \binom{w}{2l'+1} = \frac{4^n}{2^w} 2^{w-1} = \frac{4^n}{2}, \quad (2.6)$$

where  $\lfloor \dots \rfloor$  denotes the integer part. It is remarkable that the number of  $\rho$  anticommuting with a given  $\sigma \neq \mathbb{1}$  does not depend on the weight of  $\sigma$ .

The commutator of two elements of the basis (if not vanishing) is proportional to another element of the basis, because the two products in the commutator give the opposite matrix ( $l$  is odd). Given two non-commuting elements of the basis  $\sigma$  and  $\tau$  we define  $q_{[\sigma,\tau]}$  as the penalty of their commutator; if  $[\sigma, \tau] = 0$  we set by definition  $q_{[\sigma,\tau]} = 1$ .

---

<sup>1</sup>This terminology is common in the quantum information literature.

## 2.2 Connection and geodesic equation

Let's now derive an expression for the Levi-Civita connection  $\nabla$  compatible with the metric (2.3). This is given by the Koszul formula [57], which, thanks to the fact that the inner product can be computed at the identity (and therefore is constant in a suitable basis), simplifies to

$$-2i\langle \nabla_X Y, Z \rangle = \langle [X, Y], Z \rangle + \langle [Z, X], Y \rangle - \langle [Y, Z], X \rangle \quad (2.7)$$

where  $X, Y, Z$  are right-invariant fields interpreted as Hermitian matrices at the origin. Eq. (2.7) allows us to define

$$\nabla_X Y = \frac{i}{2} ([X, Y] + \mathcal{G}^{-1}([X, \mathcal{G}(Y)] + [Y, \mathcal{G}(X)])) . \quad (2.8)$$

Setting  $Y = X$  in eq. (2.8), we obtain the geodesic equation, which is nothing but the Euler-Arnold equation [56]:

$$\dot{X} + i\mathcal{G}^{-1}([X, \mathcal{G}(X)]) = 0 . \quad (2.9)$$

In general we expect that geodesics have an intricate behaviour. Eq. (2.9) shows that there exists a simple class of geodesics, given by the exponential of an eigenvector of the penalty operator  $\mathcal{G}$ .

## 2.3 Riemann tensor

Let's now specialize the discussion to  $SU(2^n)$  using Pauli matrices  $\rho, \sigma, \tau, \mu$ , which can be viewed as are right-invariant frame fields. The curvature tensor is [5]

$$R_{\rho\sigma\tau\mu} = \langle \nabla_\rho \tau, \nabla_\sigma \mu \rangle - \langle \nabla_\sigma \tau, \nabla_\rho \mu \rangle - \langle \nabla_{i[\rho, \sigma]} \tau, \mu \rangle . \quad (2.10)$$

Using eq. (2.8), we find:

$$\nabla_\sigma \tau = i c_{\sigma, \tau} [\sigma, \tau] , \quad c_{\sigma, \tau} \equiv \frac{1}{2} \left( 1 + \frac{q_\tau - q_\sigma}{q_{[\sigma, \tau]}} \right) . \quad (2.11)$$

The Riemann tensor is given by the expression:

$$R_{\rho\sigma\tau\mu} = c_{\rho, \tau} c_{\sigma, \mu} \langle i[\rho, \tau], i[\sigma, \mu] \rangle - c_{\sigma, \tau} c_{\rho, \mu} \langle i[\sigma, \tau], i[\rho, \mu] \rangle - c_{[\rho, \sigma], \tau} \langle i[i[\rho, \sigma], \tau], \mu \rangle . \quad (2.12)$$

Since eq. (2.12) depends just on commutators, the Riemann curvature of a subgroup of unitaries does not depend on the metric data outside this subgroup. For example, complexity on a one qubit subgroup depends just on penalties of generators acting on that particular subgroup. An important result [5] is that the component  $R_{\rho\sigma\tau\mu}$  vanishes unless the product of the corresponding generalized Pauli matrices  $\rho\sigma\tau\mu$  is proportional to the identity.

## 2.4 Sectional curvatures

The sectional curvature is defined as half of the scalar curvature of a 2-dimensional submanifold with tangent space specified by the directions  $(\rho, \sigma)$ . The general expression for the sectional curvature of the plane determined by the vectors  $(v, w)$  is [58]

$$K(v, w) = \frac{R_{\alpha\beta\gamma\delta} v^\alpha w^\beta w^\gamma v^\delta}{(v_\alpha v^\alpha)(w_\beta w^\beta) - (v_\alpha w^\alpha)^2} . \quad (2.13)$$

The quantity  $K(v, w)$  depends just on the plane which is defined by  $(v, w)$  and does not depend on their normalisation. Sectional curvature is a non-linear object and it is a non

trivial function of the orientation of the plane; in general, in order to determine  $K$  on an arbitrary plane it is not enough to determine it on the planes defined by couples of vectors on an orthogonal basis.

The generalized Pauli matrices are orthogonal but not normalized, see eq. (2.4). The sectional curvature in the plane spanned by two generalized Pauli matrices is

$$K(\rho, \sigma) = \frac{R_{\rho\sigma\sigma\rho}}{q_\rho q_\sigma}. \quad (2.14)$$

From eq. (2.12) we find

$$R_{\rho\sigma\sigma\rho} = c_{\rho,\sigma} c_{\sigma,\rho} \langle i[\rho, \sigma], i[\sigma, \rho] \rangle - c_{[\rho,\sigma],\sigma} \langle i[i[\rho, \sigma], \sigma], \rho \rangle. \quad (2.15)$$

A direct calculation gives:

$$\langle i[\rho, \sigma], i[\rho, \sigma] \rangle = 4q_{[\rho,\sigma]}, \quad \langle i[i[\rho, \sigma], \sigma], \rho \rangle = -4q_\rho, \quad (2.16)$$

where in both the relations we repeatedly use the fact that  $\rho$  and  $\sigma$  anticommute. We can also use the property  $q_{[[\rho,\sigma],\sigma]} = q_\rho$  to get the sectional curvature

$$K(\rho, \sigma) = \frac{1}{q_\rho q_\sigma} \left[ -3q_{[\rho,\sigma]} + 2(q_\rho + q_\sigma) + \frac{(q_\rho - q_\sigma)^2}{q_{[\rho,\sigma]}} \right], \quad (2.17)$$

which is valid if  $[\rho, \sigma] \neq 0$  (otherwise  $K(\rho, \sigma) = 0$ ).

This formula, which as far as we know is new and not contained in [5], has interesting consequences. We see that the only negative contribution to  $K(\rho, \sigma)$  comes from  $q_{[\rho,\sigma]}$ :  $K$  can become negative just if the commutator  $[\rho, \sigma]$  has a large enough penalty factor. In general, we expect that  $K$  is positive, unless  $q_{[\rho,\sigma]}$  is big enough compared to  $q_\rho$  and  $q_\sigma$ .

One may wonder if it is possible to get negative all the sectional curvatures of the orthogonal basis. This is not possible, because the  $K$  of the one qubit subspace depend just on the one qubit penalty factors. In Section 3 we will show that at least 2 out of 3 independent sectional curvatures are always positive for one qubit.

## 2.5 Ricci tensor and curvature

Sectional curvatures are related to Ricci tensor and Ricci curvature. Given an orthonormal basis  $\{e_k\}$  with  $k = 1, \dots, N$  and such that  $e_1 = v$ , we have the following result [58] valid for all Riemannian manifolds:

$$R_{\alpha\beta} v^\alpha v^\beta = \sum_{k=2}^N K(v, e_k). \quad (2.18)$$

In this way the scalar curvature can be expressed in terms of the sectional curvatures as

$$R = \sum_{k=1}^N R_{\alpha\beta} e_k^\alpha e_k^\beta = \sum_{\sigma, \rho} K(\rho, \sigma). \quad (2.19)$$

It should be emphasised that the sectional curvatures do not transform linearly as tensors, still their sum reproduces the Ricci scalar.

The sign of sectional curvatures plays a key role in relation to ergodicity [47]. Roughly speaking, the geodesic flow is called ergodic if its typical geodesic will eventually pass nearby to all the allowed portions of the operator space. The average of observables along the geodesic trajectory will then coincide with the average over the manifold of unitaries.

In the context of the motion in the group manifold of unitaries, one can consider the time evolution of two neighboring geodesics intersecting at  $t = 0$  under infinitesimally close local Hamiltonians. In such case, the deviation between the geodesics is governed by the sectional curvature corresponding to the section containing the two geodesics: if the sign is positive as in the standard inner product metric, then geodesics converge. On the other hand, an appropriate choice of penalty factors allows to obtain negative sectional curvatures which imply that the geodesics diverge. The divergence of geodesics is an important requirement for quantum chaos, which in turn requires an ergodic behaviour.

From a general theorem [51], we know that geodesic flow is ergodic in manifolds whose all sectional curvatures are negative. This result is not directly applicable to unitary complexity, because at least some of the sectional curvatures in the one qubit directions are always positive. Indeed, ergodicity of geodesic is still preserved in some examples where the curvature is partly negative and partly positive (see e.g. [59]). In general, we expect that the presence of directions with mostly negative sectional curvatures is a strong indication of ergodic behaviour of geodesics. From eq. (2.19) we know that the scalar curvature is the sum of all sectional curvature of an orthogonal basis, and so we expect that negative scalar curvature  $R$  is a detector of ergodicity. Unfortunately we don't know about any rigorous mathematical theorem which relates the sign of  $R$  to the ergodicity of geodesics.

In view of the investigation of conjugate points of the geodesics in Section 6, it is convenient to introduce a specific notation for the diagonal components of the Ricci tensor. Using an orthonormal basis  $\{u(\sigma)\}$  in the algebra, we define

$$R_\sigma = R_{\alpha\beta} u^\alpha(\sigma) u^\beta(\sigma) = \frac{R_{\sigma\sigma}}{q_\sigma}, \quad u^\alpha(\sigma) u^\beta(\sigma) g_{\alpha\beta} = 1. \quad (2.20)$$

Using the definitions for the curvature quantities given above, we start considering in Section 3 the simple cases where the quantum-mechanical system is composed by one or two qubits. We will extract the sectional curvatures and the Ricci scalar and study their behaviour in relation to various choices of the penalty factors on the generators. Then we will generalize in Section 4 to the case with many qubits, where we will propose some choices of penalty factors to reproduce expected properties of complexity.

### 3 Few qubits examples

#### 3.1 One qubit

Let us fix the penalty factor for  $\sigma_x$  to 1, and denote the penalty factors for  $\sigma_y$  and  $\sigma_z$  by  $Q$  and  $P$ . For  $Q = 1$ , the metric has a  $U(1)$  isotropic symmetry which rotates  $(\sigma_x, \sigma_y)$ . Applying the results of the previous section, the sectional curvatures of the planes selected by our orthonormal basis are:

$$\begin{aligned} K(\sigma_x, \sigma_y) &= \frac{-3P^2 + 2P + 2PQ + Q^2 + 1 - 2Q}{PQ}, \\ K(\sigma_x, \sigma_z) &= \frac{-3Q^2 + 2Q + 2PQ + P^2 + 1 - 2P}{PQ}, \\ K(\sigma_y, \sigma_z) &= \frac{-3 + 2P + 2Q + P^2 + Q^2 - 2PQ}{PQ}, \end{aligned} \quad (3.1)$$

and the scalar curvature is

$$R = -2 \frac{(Q - P)^2 - 2(P + Q) + 1}{PQ}. \quad (3.2)$$

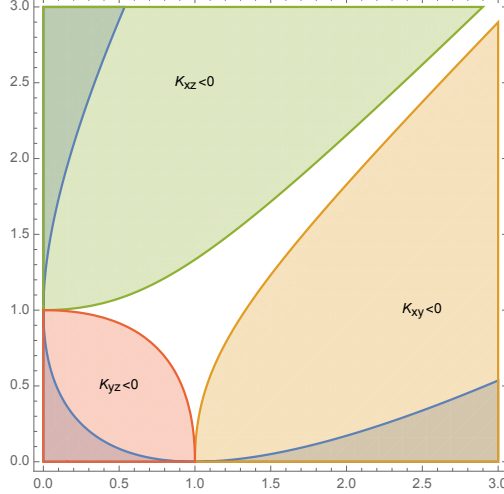


Figure 1: Regions of negativity of sectional curvatures in the  $(P, Q)$  plane. In the white region all the sectional curvatures are positive. The blue shaded regions correspond to a negative scalar curvature.

The signs of sectional and scalar curvatures are shown in Fig. 1. Note that two out of the three sectional curvatures in eq. (3.1) are positive in all the parameter space.

The sectional curvatures form a non-linear object; these quantities are not enough to compute sectional curvature in an arbitrary plane, which can be found using expressions from the Riemann tensor. In the one qubit case, we checked that the values in eq. (3.1) correspond for all  $P, Q$  to the maxima and minima of the sectional curvature.

Conventionally, we will call the generators with lowest penalty "easy" generators, and those with highest penalty "hard" generators. We are interested in limits where the maximal complexity becomes large, in general exponential in the number of states. So it might seem a contradiction to search for limits of large complexity in the one qubit Hilbert space. This is not necessarily the case: in order to explore a toy model with large maximal complexity, one may consider the limit where the weight factors  $P, Q$  go to infinity.

One of these limits may be obtained by setting

$$P = 1, \quad Q \rightarrow \infty. \quad (3.3)$$

In this case the scalar and the sectional curvatures diverge:

$$R = 8 - 2Q, \quad K(\sigma_x, \sigma_y) = 4 - 3Q, \quad K(\sigma_x, \sigma_z) = K(\sigma_y, \sigma_z) = Q. \quad (3.4)$$

In general, if we set  $P$  constant and we send  $Q \rightarrow \infty$ , we do not obtain a smooth limit.

It is also interesting to consider the limit

$$P = Q \rightarrow \infty. \quad (3.5)$$

The scalar curvature remains small:

$$R = \frac{8}{P} - \frac{2}{P^2}, \quad K(\sigma_x, \sigma_y) = K(\sigma_x, \sigma_z) = \frac{1}{P^2}, \quad K(\sigma_y, \sigma_z) = \frac{4}{P} - \frac{3}{P^2}. \quad (3.6)$$

In this case all the sectional curvatures are positive and become small.

Another possibility is to consider

$$P = \beta Q \rightarrow \infty, \quad (3.7)$$

with  $\beta$  constant. In this case at large  $\beta$  we find that the sectional curvatures approach to constants. For  $\beta \neq 1$ , at large  $P$  the scalar curvature is negative,  $R = -2(\beta - 1)^2$

In all these limits the volume of the space (measured using the complexity metric) goes to infinity. From the point of view of complexity, instead, these limits are very different. In the case (3.3) the maximal complexity does not approach infinity, because the remaining easy generators are enough to build whatever unitary we want. Instead, in the cases in eq. (3.5) and (3.7) the maximal complexity goes to infinity, because the only easy generator at our disposal allows to produce just a very special class of unitary, i.e. the rotations along the  $x$  axis.

### 3.2 Two qubits

The two qubits case is the simplest environment where we can address the question of what happens if one penalizes operators according to the number of qubits that are entangled at the same time.

We choose  $A$  as penalty factor for the weight 1 matrices and  $B$  as penalty factor for the weight 2 ones. The non-vanishing sectional curvatures  $K(\sigma, \rho)$  in the orthonormal basis can take three values:

$$a = \frac{1}{A}, \quad b = \frac{A}{B^2}, \quad c = \frac{4B - 3A}{B^2}. \quad (3.8)$$

The value  $a$  arises when  $(\sigma, \rho)$  have both weight  $w = 1$ , the value  $c$  when they have both  $w = 2$  and the value  $b$  if they are generators with different weights. The multiplicity of each value of sectional curvatures is:

$$N_a = 12, \quad N_b = 72, \quad N_c = 36. \quad (3.9)$$

The scalar curvature is:

$$R = -12 \frac{3A^2 - 12AB - B^2}{AB^2}. \quad (3.10)$$

Let us specialise  $A = 1$  and  $B = q$  with  $q > 1$ . We are penalising the weight 2 matrices (denoted as "hard") compared to the weight 1 matrices (denotes as "easy"). The scalar curvature is

$$R = 12 \frac{-3 + 12q + q^2}{q^2}, \quad (3.11)$$

which is always positive. Note that in this case the structure of the algebra generators is as follows

$$[\text{easy}, \text{easy}] = \text{easy}, \quad [\text{easy}, \text{hard}] = \text{hard}, \quad [\text{hard}, \text{hard}] = \text{easy}, \quad (3.12)$$

and so it gives rise to positive sectional curvatures, from eq. (2.17). Although such a choice is the most intuitive, it necessarily provides positive curvatures, see also [52] for the same conclusion. Note that no singularity appears in curvature if we send  $q \rightarrow \infty$ .

If we instead set  $A = p$  and  $B = 1$ , we are penalizing the weight 1 matrices and the scalar curvature is

$$R = -12 \frac{3p^2 - 12p - 1}{p}. \quad (3.13)$$

Note that in this case the structure of the algebra generators is reversed

$$[\text{hard}, \text{hard}] = \text{hard}, \quad [\text{easy}, \text{hard}] = \text{easy}, \quad [\text{easy}, \text{easy}] = \text{hard}, \quad (3.14)$$

and indeed gives negative curvature at large enough  $p$ , according to eq. (2.17). This result gives a quantitative explanation of some intuitions discussed in [52].

We point out that the abovementioned case is not the only one where such a behaviour occurs. In general, when we split the set of generators in two classes, one of which is a maximal subalgebra, the structure of commutators (3.12) and (3.14) always arises.

## 4 Many qubits

We consider quantum systems composed by many qubits, which is the first step in the direction of a system with infinite degrees of freedom as field theory. In this case it is possible to study the dependence of the curvatures on the number of qubits, in order to understand the assignment of penalty factors that can reproduce physical phenomena like the switchback effect and scrambling.

The idea is to study the time evolution of complexity when the system of interest is subject to a perturbation. From the holographic point of view, this is usually performed with the introduction of a shock wave very far in the past, in such a way that the scrambling time corresponds to the delay after which the black hole reaches again the equilibrium [7]. From the perspective of quantum circuits, a useful model consists in the evolution of an epidemic [10]. If there is a single infected qubit which can interact with all the other ones via a local Hamiltonian, the scrambling time measures the scale after which the infection has involved a large enough number of qubits in order for complexity to reach the value  $n$ , corresponding to the number of qubits.

In this context, a related effect is the switchback one, which is a delay in the growth of complexity arising from cancellations between multiple shock waves or perturbations. Using the toy model introduced in [46], it was suggested that, in order to get a satisfying description of switchback effect and scrambling, the typical sectional curvatures should scale as  $1/n$  or  $1/n^2$  in the large number of qubit limit (depending on the variant of the model). For a recent discussion of the switchback effect for low number of qubits, see [60]. Even without restricting to a particular toy model, the divergence of sectional curvatures in the large number of qubits limit gives rise to a singular behaviour that should be avoided. In this Section we will study the consequences of various assignments of penalties on the behaviour of curvatures.

### 4.1 Counting non-vanishing sectional curvatures

Let us consider the case with  $n$  qubits, equipped with a class of penalty factors which are functions just of the weight of the generators. Let us denote the penalty associated to the weight  $k$  by  $q_k$ . The number of generalised Pauli matrices with weight  $k$  in our basis is given by:

$$\mathcal{N}_k = 3^k \binom{n}{k}. \quad (4.1)$$

Given two generators  $(\rho, \sigma)$ , we have defined  $l$  as the number of corresponding tensorial product entries in which  $\rho$  and  $\sigma$  have different Pauli matrices (for anticommuting  $\rho$  and  $\sigma$ ,  $l$  is odd). We define  $m$  as the number of corresponding tensorial product entries in which  $\rho$  and  $\sigma$  have the same Pauli matrices. Let us denote respectively by  $M$  and  $N$  the weights of  $\rho$  and  $\sigma$ . We have that the number of entries in the tensorial product in which there is a Pauli matrix in  $\sigma$  and an identity in the corresponding entry in  $\rho$  is given by

$$s = N - l - m. \quad (4.2)$$

Due to the properties of generalized Pauli matrices, if a pair of generators in the basis do not commute, then they necessarily need to anti-commute. Consequently, the commutator  $[\rho, \sigma]$  has weight

$$w = M + N - l - 2m, \quad (4.3)$$

where  $l + m \leq \min(M, N)$ . The minimal weight is realised just for  $l = 1$  and for  $m = \min(N - 1, M - 1)$ . The maximum weight instead is realised by  $l = 1$  and  $m = 0$ .

In order to parameterize the possible values of the weight  $w$ , let us introduce an integer label  $r$ :

$$\begin{aligned} \text{for } N \leq M, \quad r &= N - \frac{l+1}{2} - m, \quad r = 0 \dots N-1, \\ \text{for } N > M, \quad r &= M - \frac{l+1}{2} - m, \quad r = 0 \dots M-1, \end{aligned} \quad (4.4)$$

in such a way that the weight of the commutator is

$$w_r = |M - N| + 1 + 2r. \quad (4.5)$$

The  $r = 0$  case corresponds to the lowest possible weight of the commutator, while the maximum of  $r$  corresponds to the maximum weight.

The weight is limited also by the number of qubits, i.e.  $w_r \leq n$ . So, for any given pair  $(M, N)$ , we must have that the integer  $r$  is in the following range:

$$\begin{aligned} \text{for } N \leq M, \quad 0 \leq r &\leq \min \left( N-1, \frac{n - |M - N| - 1}{2} \right), \\ \text{for } N > M, \quad 0 \leq r &\leq \min \left( M-1, \frac{n - |M - N| - 1}{2} \right). \end{aligned} \quad (4.6)$$

Note that for each fixed number of qubits  $n$ ,  $r \leq [(n-1)/2]$  where  $[\dots]$  denotes the integer part.

If two directions in the unitary space do not commute, the sectional curvatures can be obtained from eq. (2.17), i.e.

$$K(M, N, r) = \frac{1}{q_M q_N} \left( -3q_{w_r} + 2(q_M + q_N) + \frac{(q_M - q_N)^2}{q_{w_r}} \right), \quad (4.7)$$

where  $K(M, N, r)$  denotes the sectional curvature of the plane spanned by generalised Pauli matrices of weights  $M$  and  $N$ , whose commutator has weight  $w_r$ , given by eq. (4.5). If two directions commute  $K(M, N, r) = 0$ ; given a generalised Pauli matrix, about one half of the other Pauli matrices in the basis commute with it, see eq. (2.6). So about one half of the total sectional curvatures vanish by construction, independently of the penalty factors.

Given a generator  $\rho$  in the basis with weight  $M$ , we similarly denote by  $\mathcal{R}(M, N, r)$  the number of generators with weight  $N$  whose commutator with  $\rho$  has a weight parameterised by a given integer  $r$ , as in eq. (4.5).

We give now an explicit formula for  $\mathcal{R}(M, N, r)$ . Let us first consider the  $N \leq M$  case and let us start with  $r = 0$ . In this case we need to determine how many  $\sigma$  will give a  $[\rho, \sigma]$  with the minimal possible weight. As stressed before, this is realised just for  $l = 1$ ,  $m = N - 1$  and  $s = 0$ . We have  $M$  places to stick the  $l = 1$  entry of  $\sigma$  (which corresponds to a different Pauli matrix compared to  $\rho$ , so there is an extra factor of 2), and then we have  $\binom{M-1}{N-1}$  ways to stick the  $m = N - 1$  entries of  $\sigma$  with the same Pauli matrix as in  $\rho$ . The number of such matrices is:

$$\mathcal{R}(M, N, 0) = 2M \binom{M-1}{N-1}. \quad (4.8)$$

Let us consider  $r = 1$ . Here in general we have two possible situations. We may have  $l = 1$ ,  $m = N - 2$ ,  $s = 1$  or instead  $l = 3$ ,  $m = N - 3$  and  $s = 0$ . In the first case, there are 3 ways to choose the Pauli matrix in  $\sigma$  which has an identity in the corresponding entry in  $\rho$ . This gives:

$$\mathcal{R}(M, N, 1) = \binom{M}{1} 2^1 \binom{M-1}{N-2} \binom{n-M}{1} 3 + \binom{M}{3} 2^3 \binom{M-3}{N-3}. \quad (4.9)$$

In the general case we have to sum over all the possible odd values of  $l$ ; it is then convenient to set  $l = 2k + 1$  with integer  $k$ . In general we have  $\binom{M}{l} 2^l$  ways to set the entries in tensor product where  $\rho$  and  $\sigma$  have different Pauli matrices,  $\binom{M-l}{m}$  ways to set the entries in such a way that  $\rho$  and  $\sigma$  have the same Pauli matrices in the corresponding entries and  $\binom{n-M}{s} 3^s$  ways to set entries in which in the corresponding elements of  $\rho$  and  $\sigma$  there are respectively an identity matrix and a Pauli matrix. The total combinatorial factors is

$$\begin{aligned}\mathcal{R}(M, N, r) &= \sum_{k=0}^r \binom{M}{l} 2^l \binom{M-l}{m} \binom{n-M}{s} 3^s \\ &= \sum_{k=0}^r \binom{M}{2k+1} 2^{2k+1} \binom{M-2k-1}{N-k-1-r} \binom{n-M}{r-k} 3^{r-k},\end{aligned}\quad (4.10)$$

where we used  $s = r - k$ . In this expression we should not worry about negative values of  $N - k - 1 - r$ , which indeed may occur, because they vanish after analitically continuing the binomial coefficients with the  $\Gamma$  function.

If  $N > M$ , we can write a similar formula. We can still use the same eq. (4.10), with  $s = r - k + N - M$ :

$$\begin{aligned}\mathcal{R}(M, N, r) &= \sum_{k=0}^r \binom{M}{l} 2^l \binom{M-l}{m} \binom{n-M}{s} 3^s \\ &= \sum_{k=0}^r \binom{M}{2k+1} 2^{2k+1} \binom{M-2k-1}{M-k-1-r} \binom{n-M}{r-k+N-M} 3^{r-k+N-M}.\end{aligned}$$

Let us denote by  $\mathcal{N}(M, N, r)$  the number of sectional curvatures with value given by eq. (4.7). These can be found as

$$\mathcal{N}(M, N, r) = \mathcal{N}_M \mathcal{R}(M, N, r) = \mathcal{N}_N \mathcal{R}(N, M, r), \quad (4.11)$$

where  $\mathcal{N}_M, \mathcal{N}_N$  are defined in eq. (4.1).

## 4.2 Draconian penalties

The combination of 1 and 2 qubits operators is universal and can be used to build an arbitrary operator in  $SU(2^n)$  [61]. This result suggests a somewhat minimal choices of penalty factors, studied in detail in [5]

$$\begin{aligned}q_\sigma &= 1, & w &\leq 2, \\ q_\sigma &= q, & w &> 2.\end{aligned}\quad (4.12)$$

This choice does not distinguish different values of the weight  $w > 2$  and was called "draconian" in [52].

The sectional curvatures can be found using the general expression in eq. (2.17), giving the values in Table 1.

For  $q = 1$  we recover the case where all the penalty factors are equal, which corresponds to a bi-invariant metric on  $SU(2^n)$ . In this case all the non-vanishing sectional curvatures are equal and positive. The interesting region with negative curvature is at large  $q$ . So in this limit it makes sense to use the approximation where only the sectional curvatures at leading order in  $q$  are considered.

Let us consider the approximation in which we keep just the  $\mathcal{O}(q)$  and the  $\mathcal{O}(1)$  terms. In this limit the only non-vanishing sectional curvatures are:

$$\begin{aligned}K(1, 1, 0) &= K(2, 1, 0) = K(2, 2, 0) = 1, \\ K(3, 2, 0) &= q, & K(2, 2, 1) &= 4 - 3q,\end{aligned}\quad (4.13)$$

	$[\rho, \sigma] \in \mathcal{P}$	$[\rho, \sigma] \in \mathcal{Q}$
$\rho, \sigma \in \mathcal{P}$	$K = 1$	$K = 4 - 3q$
$\rho, \sigma \in \mathcal{Q}$	$K = \frac{4q-3}{q^2}$	$K = \frac{1}{q}$
$\rho \in \mathcal{P}, \sigma \in \mathcal{Q}$	$K = q$	$K = \frac{1}{q^2}$

Table 1: Values of the non-vanishing sectional curvature  $K$  for various choices of  $\rho, \sigma$  in the model with draconian penalty factors. We denote by  $\mathcal{P}$  and  $\mathcal{Q}$  respectively the set of generators with  $w \leq 2$  and  $w > 2$ .

with multiplicities

$$\begin{aligned} \mathcal{N}(1, 1, 0) &= 6n, & \mathcal{N}(2, 1, 0) &= \mathcal{N}(2, 2, 0) = 18n(n-1), \\ \mathcal{N}(3, 2, 0) &= \mathcal{N}(2, 2, 1) = 54n(n-1)(n-2). \end{aligned} \quad (4.14)$$

The scalar curvature then is:

$$R = -54n(n-1)(n-2)q + 6n(36n^2 - 99n + 64). \quad (4.15)$$

This calculation is in agreement with the exact result computed in [5] in a different way:

$$\begin{aligned} R &= -54qn(n-1)(n-2) + 6n[36n^2 - 99n + 64] + \\ &+ \frac{1}{q} \left[ \frac{4^n}{2} \left( 4^n - 1 + \frac{3n(3n-1)}{2} \right) - 6n(45n^2 - 117n + 74) \right] + \\ &- \frac{1}{q^2} [3n(3n-1)4^{n-1} - 6n(3n-4)(6n-7)]. \end{aligned} \quad (4.16)$$

In order to get negative curvature, we need  $q \propto 4^n$  or larger. This means that  $q$  has to grow exponentially with  $n$ . In particular, in this regime the scalar curvature is dominated by a small number (polynomial in  $n$ ) of sectional curvatures whose magnitude grows like  $|K| \approx q \approx 4^n$ . This is a singular limit, and, as discussed in [47], this brings to some unwanted properties in the scrambling and switchback effect of black holes complexity.

### 4.3 Towards a more sustainable taxation policy

In [47] a more moderate penalty factor was advocated:

$$\begin{aligned} q_\sigma &= 1, & w &\leq 2, \\ q_\sigma &= c4^{w-2}, & w &> 2, \end{aligned} \quad (4.17)$$

where  $c$  is an order 1 constant. The authors called this choice "moderate", because sectional curvatures are not as big as in the draconian model. Big curvatures in general are not a desired feature of complexity geometry, because they are in tension with the desired properties of scrambling and switchback effect. The exponential behaviour  $q_k \propto 4^k$  in (4.17) is suggested by the draconian model: in such case the behaviour  $q \propto 4^n$  of penalties is needed in order to have negative curvature. In this section we will consider some variations of this model, in which  $q_k \propto \alpha^k$  for some appropriate constant  $\alpha$ .

The draconian model resembles a flat tax: all the weights bigger than 2 are treated the same. The middle-class exponents with  $w \approx 3$  and the billionaires with  $w \approx n$  pay exactly the same amount of taxes. The penalty choice in eq. (4.17) goes in the direction of a more progressive taxation, because high incomes are taxed progressively. Still there is a minor source of inequality in eq. (4.17): the very low income guys at  $w = 1$  are taxed just the

same as the working class at  $w = 2$ . In order to promote social justice we are motivated to introduce the following choice of penalties (see also [62])

$$q_\sigma = \alpha^{w(\sigma)-1}, \quad (4.18)$$

which we will call "progressive" penalties. The scaling as  $4^k$  at large  $k$  is generalised as  $\alpha^k$ .

The model (4.18) simplifies in the large  $\alpha$  limit, which can be used as an expansion parameter for the analytical understanding of the model. In particular, from eq. (2.17) we can see that at large  $\alpha$  sectional curvatures scale at most as  $\alpha^0$ . With the choice in eq. (4.18), we expect that by construction the maximal complexity becomes infinity at fixed  $n$  in the limit  $\alpha \rightarrow \infty$ , because one qubit operators can not produce the most general operators in the unitary space. For example, they cannot produce unitaries which entangle two qubits which were previously unentangled. Physically, we will be interested in the limit of large but finite  $\alpha$ .

Moreover, we can consider generalisations of this basic model. In particular, we can generalise the choice in eq. (4.18) as

$$\begin{aligned} q_\sigma &= 1, & w &\leq w_0, \\ q_\sigma &= \alpha^{w-w_0}, & w &> w_0, \end{aligned} \quad (4.19)$$

with  $w_0 \geq 2$ . For  $w_0 = 2$  and  $\alpha = 4$ , we recover the model studied in [47]. We will refer to this model as moderate model with threshold  $w_0$ . With this choice of penalties, we expect that the maximal complexity at fixed  $n$  does not diverge for  $\alpha \rightarrow \infty$ , because the combination of 1 and 2 qubits operators is universal and can be used to build an arbitrary operator in the unitary space. From eq. (2.17), we can see that this model has the property that at large  $\alpha$  sectional curvatures scale at most as  $\alpha^{w_0-1}$ . Therefore, the large  $\alpha$  limit provides a singular geometry, as the curvature diverges.

#### 4.4 Progressive penalties

In this section we consider the choice in eq. (4.18). A direct calculation gives, for  $N \leq M$ :

$$K(M, N, r) = -3\alpha^{2(r+1-N)} + 2\alpha^{1-N} + 2\alpha^{1-M} + \alpha^{-2r}(1 + \alpha^{-2(M-N)} - 2\alpha^{-(M-N)}), \quad (4.20)$$

and, for  $N > M$ :

$$K(M, N, r) = -3\alpha^{2(r+1-M)} + 2\alpha^{1-N} + 2\alpha^{1-M} + \alpha^{-2r}(1 + \alpha^{-2(N-M)} - 2\alpha^{-(N-M)}). \quad (4.21)$$

Note that at large  $\alpha$  sectional curvatures scale at most as  $\alpha^0 + \mathcal{O}(\alpha^{-1})$ . Let us start with the  $\alpha^0$  terms.

For  $r = 0$ , the only non-vanishing sectional curvatures at this order are  $K = 1$ , for  $M = N = 1$  and

$$M, N > 1, \quad M \neq N. \quad (4.22)$$

For  $r \geq 1$ , the only term that can be of order  $\alpha^0$  is for  $M, N > 1$  and is given by

$$K(M, N, r) = \begin{cases} -3\alpha^{2(r+1-N)} + \mathcal{O}(\alpha^{-1}) & M \geq N \\ -3\alpha^{2(r+1-M)} + \mathcal{O}(\alpha^{-1}) & M < N \end{cases}. \quad (4.23)$$

If  $M \geq N$ , we have  $r = 0, \dots, N-1$ , then  $K = -3$  only for the maximal value  $r = N-1$ . If  $M < N$ , we have  $r = 0, \dots, M-1$ , then  $K = -3$  only for the maximal value  $r = M-1$ .

We first compute the Ricci tensor contracted with a unit vector  $\sigma$  with weight  $M$ , as defined in eq. (2.20):

$$R_M = \sum_N \sum_r K(M, N, r) \mathcal{R}(M, N, r). \quad (4.24)$$

For  $M = 1$ , the only leading-order contribution is for  $M = N = 1$ :

$$R_1 = \mathcal{R}(1, 1, 0) = 2. \quad (4.25)$$

Let us now consider  $1 < M \leq n$ . The positive leading-order contributions to  $R_M$  are given by the scalar curvatures with  $r = 0$ , whose value is  $K = 1$ :

$$R_M^+ = \sum_{N=2}^{M-1} \mathcal{R}(M, N, 0) + \sum_{N=M+1}^n \mathcal{R}(M, N, 0) = 2M \left( 2^{M-1} - 3 + 2^{2(n-M)} \right). \quad (4.26)$$

The negative leading-order contributions to  $R_M$  are given by the scalar curvatures with  $r = N - 1$  if  $M \geq N$  and  $r = M - 1$  if  $M < N$ , all equal to  $K = -3$ . The expression turns out to be the same for both the cases:

$$\begin{aligned} \mathcal{R}(M, N, N-1) &= 2M \binom{n-M}{N-1} 3^{N-1}, & M \geq N \\ \mathcal{R}(M, N, M-1) &= 2M \binom{n-M}{N-1} 3^{N-1}, & M < N. \end{aligned} \quad (4.27)$$

We finally get

$$\begin{aligned} R_M^- &= -3 \left( \sum_{N=2}^M \mathcal{R}(M, N, N-1) + \sum_{N=M+1}^{N_{\max}} \mathcal{R}(M, N, M-1) \right) \\ &= \sum_{N=2}^{1+n-M} 2M \binom{n-M}{N-1} 3^{N-1} = -6M \left[ 2^{2(n-M)} - 1 \right]. \end{aligned} \quad (4.28)$$

The maximum value of  $N$  in the sum,  $N_{\max} = 1 + n - M$ , ensures that  $r = M - 1$  is allowed in the case  $M < N$ , as can be obtained from eq. (4.6).

The final result for  $R_M$  at the leading order is:

$$R_M = R_M^+ + R_M^- = 2M \left( 2^{M-1} - 2^{2(n-M)+1} \right). \quad (4.29)$$

Using eq. (4.1) and this result, the scalar curvature is computed as

$$R = \sum_{M=1}^n \mathcal{N}_M R_M = 3n (4^n - 2 \cdot 7^{n-1}). \quad (4.30)$$

The scalar curvature is negative for  $n \geq 3$  and comes just from two values of the sectional curvatures:  $K = 1$  with multiplicity  $\mathcal{N}_+$  and  $K = -3$  with multiplicity  $\mathcal{N}_-$ , where

$$\mathcal{N}_+ = 12 \cdot 7^{n-1} n - 3 \cdot 2^{2n+1} n + 18n, \quad \mathcal{N}_- = \frac{\mathcal{N}_+}{2} - 3n, \quad (4.31)$$

We can systematically improve this calculation order by order in the expansion parameter  $\alpha$ . For example, at order  $\alpha^{-1}$ , the only non-zero contribution to the sectional

curvature, that we denote as  $\delta K(M, N, r)$ , are

$$\begin{aligned}
M &= N = 2, & r &= 0, 1, & \delta K &= \frac{4}{\alpha}, \\
M &= N + 1, & N &\geq 3, & r &= 0, & \delta K &= -\frac{2}{\alpha}, \\
M &= 2, & N &\geq 4, & r &= 0, & \delta K &= \frac{2}{\alpha}, \\
M &= 2, & N &\geq 3, & r &= 1, & \delta K &= \frac{2}{\alpha},
\end{aligned} \tag{4.32}$$

and the ones obtained exchanging  $M$  with  $N$ . Due to a non-trivial cancellation, the only corrections to  $R_M$  is for  $w = 2$

$$\delta R_2 = \frac{4^n}{\alpha}. \tag{4.33}$$

This gives the following correction to the curvature

$$\delta R = \frac{9}{2} n(n-1) \frac{4^n}{\alpha}. \tag{4.34}$$

In order to get a feeling on the average sectional curvature, it is convenient to divide  $R$  by the total number of sectional curvatures between couples of elements in the basis, which we denote by

$$\eta = (4^n - 1)^2 - (4^n - 1). \tag{4.35}$$

The average sectional curvature becomes tiny at large  $n$  and  $\alpha$ , i.e.

$$\bar{K} = \frac{R}{\eta} \approx -\frac{6}{7} n \left( \frac{7}{16} \right)^n + \frac{1}{\alpha} \frac{9}{4^n} \frac{n(n-1)}{2}. \tag{4.36}$$

The average sectional curvature as a function of  $\alpha$  for a few values of  $n$  is plotted in Fig. 2. Nothing special happens for the value  $\alpha = 4$ , which instead plays an important role for the draconian model. It is interesting that there is a minimum at finite  $\alpha$ . It turns out that the series expansion in  $\alpha^{-1}$  for  $\bar{K}$  is, at large  $n$ , an alternate sign series with slow rate of convergence. For example, in order to get the minimum in the plot for  $\bar{K}$  when  $n = 10$ , we have to expand up to the order  $\alpha^{-5}$ .

This choice of penalties for  $\alpha \rightarrow \infty$  has many similarities with the one qubit case in eq. (3.7), where  $P = \beta Q \rightarrow \infty$  with  $\beta$  constant and different from 1. In both limits we expect that the maximal complexity diverges, and the sectional curvatures do not. Also  $R$  approaches a negative constant in both cases.

## 5 State complexity and submersions

Up to now, we have focused the discussion on the complexity of *unitaries*. In this section, we bring the attention of our reader to the geometry of the space of *states*. Geometrically, this space is naturally associated with a quotient of the space of unitaries, where all the different unitary transformations that, starting from a given reference state, build the same state (up to a phase) are identified. The complexity of the state built in this way is then defined to be the minimum of the complexities of all the identified unitaries. Requiring that the state complexity is also obtained as a length on the space of states defines a map between two Riemannian manifolds, which turns out to be a *Riemannian submersion*. We recall its definition in Section (5.1), and we proceed in the subsequent sections in exploiting known results for Riemannian submersions.

In particular, O'Neill's formula relates the curvature of the space of states to the curvature of the space of unitaries, providing a lower bound on the curvature on states. This underlying geometrical structure allows a direct comparison of some class of geodesics, which we explore in Section 5.6 and 6.

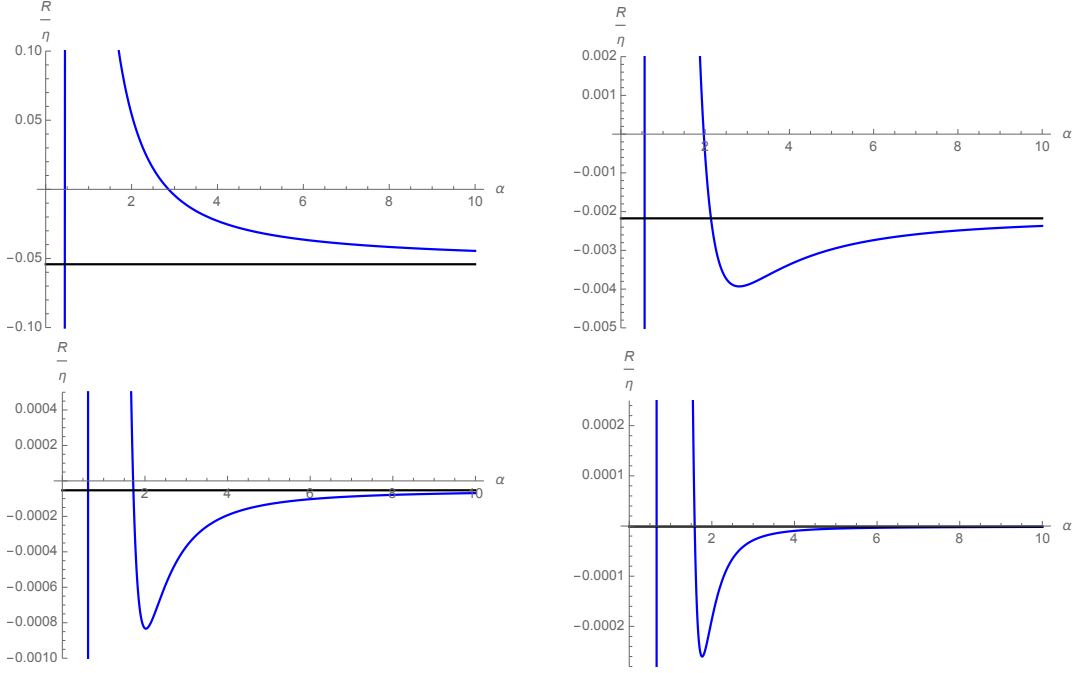


Figure 2:  $R/\eta$  as a function of  $\alpha$  in the case of moderate penalties, for  $n = 5, 10, 15, 20$ . The asymptotic value at  $\alpha \rightarrow \infty$  is shown in black. The minimum in the picture appears for  $n \geq 8$ . Increasing  $n$ , the shape of the minimum tends to become more and more steep and it is located at a lower value of  $\alpha$ .

## 5.1 Submersions

For convenience of the reader, in this section we briefly review the concept of Riemannian submersions, referring to the textbooks [57, 63] for more details.

Let us consider two Riemannian manifolds  $(M, g_{\alpha\beta})$  with dimension  $m$  and  $(B, h_{\alpha\beta})$  with dimension  $b < m$  and a smooth map  $\pi : M \rightarrow B$  with surjective differential  $d\pi$ .  $d\pi$  is a map  $d\pi : TM \rightarrow TB$ , that for any  $y \in M$  induces a linear map between the vector spaces  $T_y M$  and  $T_x B$ , where  $x = \pi(y)$ . This map has maximal rank, and thus a kernel of dimension  $f = m - b$ . We will call  $\mathcal{V}_y = \ker(d\pi_y)$  the *vertical space at y*. Its orthogonal complement in  $T_y M$ , induced by the metric  $g$ , is called the *horizontal space at y* and denoted by  $\mathcal{H}_y$ . For the submersion to be Riemannian,  $\mathcal{H}_y$  is identified with  $T_x B$  in an isometric way, in other words

$$g(X, Y) = h(d\pi(X), d\pi(Y)), \quad \forall X, Y \in \mathcal{H}_y. \quad (5.1)$$

A pictorial depiction is shown in Figure 3.

Quotients of manifolds by an isometric group action provide interesting examples of submersion (see for example the textbooks [57, 63]). Let  $M$  be a Riemannian manifold and  $G$  be a closed subgroup of the isometry group of  $M$ , and denote by  $\pi$  the projection from  $M$  to the quotient space  $B = M/G$ . This defines a natural metric on  $B$  such that  $\pi$  is a Riemannian submersion [57].

In the following sections, we make use of this construction to understand properties of the space of states from the complexity of unitaries.

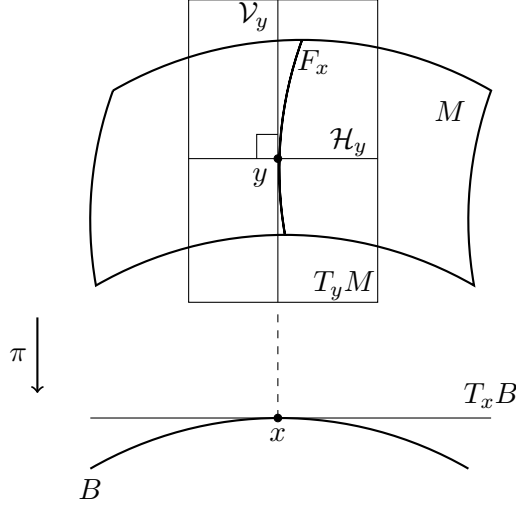


Figure 3: A reproduction of a depiction of a submersion from [63].

## 5.2 Submersions and complexity geometry

Let us apply the notion of submersion to the complexity geometry. We take  $M = SU(2^n)$  with a right-invariant metric (the unitary space) and  $G$  as the subgroup of the isometries of  $M$  which leaves the reference state invariant up to a phase. Precisely, we consider a unitary  $U$  which generates the state  $|\psi\rangle$  starting from the reference state  $|\psi_0\rangle$

$$U|\psi_0\rangle = |\psi\rangle. \quad (5.2)$$

We call *unbroken subgroup* the subgroup of  $SU(2^n)$  that fixes the reference state up to a phase

$$V|\psi_0\rangle = e^{i\phi}|\psi_0\rangle. \quad (5.3)$$

Such a  $V$  is an element of  $SU(2^n - 1) \times U(1)$ . Thus, up to a phase, both  $U' \equiv UV$  and  $U$  prepare the same state  $|\psi\rangle$ :

$$U'|\psi_0\rangle = e^{i\phi}|\psi\rangle, \quad \implies \quad U' \sim U. \quad (5.4)$$

Therefore we have a map from the unitary space to the quotient  $B$  defined as

$$\pi : \quad SU(2^n) \rightarrow B = \mathbb{CP}^{2^n-1} = \frac{SU(2^n)}{SU(2^n - 1) \times U(1)}. \quad (5.5)$$

This map is an isometric submersion, as we are going to prove writing it explicitly in a specific coordinate system.

In order to make contact with Section 2, we take a diagonal penalty matrix in the basis of the generalized Pauli matrices, see eq. (2.4), with the property

$$\langle \sigma_r, \sigma_s \rangle = q_r \delta_{rs} = q_r \frac{1}{2^n} \text{Tr}(\sigma_r \sigma_s). \quad (5.6)$$

For the states metric it is more convenient to do a change of basis. We can identify a basis for broken generators  $\rho_k$  and unbroken ones  $\tau_a$ :

$$\omega_l = (\rho_k, \tau_a), \quad 1 \leq k \leq 2(K-1), \quad 1 \leq a \leq (K-1)^2, \quad K = 2^n, \quad (5.7)$$

with normalization

$$\text{Tr}(\omega_l \omega_m) = \delta_{ml}. \quad (5.8)$$

We can express

$$\sigma_r = \sum_l \omega_l \text{Tr}(\omega_l \sigma_r), \quad \omega_l = \frac{1}{2^n} \sum_r \sigma_r \text{Tr}(\omega_l \sigma_r). \quad (5.9)$$

Then we can find the penalty scalar product in the basis  $\omega^k$ :

$$M_{lm} = \langle \omega_l, \omega_m \rangle = \frac{1}{2^{2n}} \sum_r q_r \text{Tr}(\omega_l \sigma_r) \text{Tr}(\omega_m \sigma_r). \quad (5.10)$$

This discussion also applies to the case where  $M_{lm}$  is a generic symmetric matrix. Let us introduce the following notation for the exponential of broken and unbroken generators

$$U_\theta = e^{i\theta_k \rho_k}, \quad V_\lambda = e^{i\lambda_a \tau_a}, \quad (5.11)$$

We can use the variables  $\theta_k$  to parameterize the state space. A generic element of  $SU(K)$  can be written as  $U = U_\theta V_\lambda$ . Then we can compute

$$dU U^\dagger = (dU_\theta V_\lambda + U_\theta dV_\lambda) V_\lambda^\dagger U_\theta^\dagger = dU_\theta U_\theta^\dagger + U_\theta dV_\lambda V_\lambda^\dagger U_\theta^\dagger, \quad (5.12)$$

where

$$dU_\theta = \frac{\partial U_\theta}{\partial \theta_k} d\theta_k, \quad dV_\lambda = \frac{\partial V_\lambda}{\partial \lambda_j} d\lambda_j. \quad (5.13)$$

We can now define the following quantities:

$$X_r = -i \text{Tr}(dU U^\dagger \omega_r) = -i (\text{Ad}_{U_\theta^\dagger})_{rs} \text{Tr} \left\{ (U_\theta^\dagger dU_\theta + dV_\lambda V_\lambda^\dagger) \omega_s \right\}. \quad (5.14)$$

where we have used the adjoint action

$$U_\theta^\dagger \omega_r U_\theta = (\text{Ad}_{U_\theta^\dagger})_{rs} \omega_s. \quad (5.15)$$

We can now write the metric in the unitary space as

$$ds^2 = M_{rs} X_r X_s = \tilde{M}_{lm} (u_l + v_l)(u_m + v_m), \quad (5.16)$$

where

$$\begin{aligned} \tilde{M}_{lm} &= M_{rs} (\text{Ad}_{U_\theta^\dagger})_{rl} (\text{Ad}_{U_\theta^\dagger})_{sm}, \\ u_s &= -i \text{Tr} \left\{ U_\theta^\dagger dU_\theta \omega_s \right\}, \quad v_s = -i \text{Tr} \left\{ dV_\lambda V_\lambda^\dagger \omega_s \right\}, \end{aligned} \quad (5.17)$$

in such a way that  $\tilde{M}_{lm}$  depends just on  $\theta_k$ ,  $u_s$  contains just  $(\theta_k, d\theta_k)$  and  $v_s$  contains just  $(\lambda_k, d\lambda_k)$ .

Now it is convenient to split the indices in  $\omega_r$  in indices corresponding to broken and unbroken generators, as in eq. (5.7). We have that  $v_i = 0$  for  $i$  corresponding to a broken index. Then we can write the unitary metric eq. (5.16) as

$$\begin{aligned} ds^2 &= \begin{pmatrix} u_i & u_a + v_a \end{pmatrix} \begin{pmatrix} \tilde{M}_{ij} & \tilde{M}_{ib} \\ \tilde{M}_{aj} & \tilde{M}_{ab} \end{pmatrix} \begin{pmatrix} u_j \\ u_b + v_b \end{pmatrix} \\ &= (\tilde{M}_{ij} - \tilde{M}_{ic} \tilde{M}_{ca}^{-1} \tilde{M}_{aj}) u_i u_j + \tilde{M}_{ab} f_a f_b, \end{aligned} \quad (5.18)$$

where we introduced

$$f_a = v_a + u_a + \tilde{M}_{ad}^{-1} \tilde{M}_{dj} u_j. \quad (5.19)$$

The problem of finding the minimal infinitesimal operator which synthesizes the states of coordinates  $\theta_k + d\theta_k$  from the state with coordinate  $\theta_k$  is then solved by the equation  $f_a = 0$ , because the term  $\tilde{M}_{ab}f_af_b$  in eq. (5.18) is positive-definite. This construction generalises the result in [52] to arbitrary number of qubits.

We can then identify the metric on the state space  $B$  as

$$ds_S^2 = (\tilde{M}_{ij} - \tilde{M}_{ic}\tilde{M}_{ca}^{-1}\tilde{M}_{aj})u_iu_j. \quad (5.20)$$

We explicitly checked that the metric in the space of states  $\mathbb{CP}^1$  for a single qubit coincides with the result found in [52]. In section 5.5 we will see how to apply this result to qutrits.

From eq. (5.18), it follows that the projection map  $\pi$  from  $M$  to  $B$

$$\pi : (\theta_k, \lambda_j) \rightarrow (\theta_k) \quad (5.21)$$

is a Riemannian submersion, where  $\pi^{-1}(\theta_k)$  is parametrised by  $\lambda_k$ , for fixed  $\theta_k$ . The explicit expression for the horizontal spaces at arbitrary  $\theta_k$  is given by  $f_a(X) = 0$  for any generic vector  $X$  in the tangent space.

### 5.3 Submersions and curvature

We can use O'Neill's formula [53] to relate the sectional curvatures of states  $K_S$  to the one of unitaries  $K$ :

$$K_S(\tilde{h}_1, \tilde{h}_2) = K(h_1, h_2) + \frac{3}{4} \frac{|\mathcal{V}([h_1, h_2])|^2}{|h_1|^2|h_2|^2 - \langle h_1, h_2 \rangle^2}, \quad (5.22)$$

where  $\mathcal{V}$  is the projector on the vertical subspace,  $\langle \dots \rangle$  is the scalar product from the metric of the manifold  $M$ ,  $|\dots|$  is the norm induced by the scalar product,  $\tilde{h}_k = d\pi(h_k)$  are vectors fields in the state space,  $h_k$  are horizontal fields in the unitary space,  $[h_1, h_2]$  is the commutator of the vector fields in the state space.

This expression shows that the sectional curvature of a plane in the space of states can be always expressed as sectional curvature of an appropriate plane in the unitary space plus a positive definite contribution coming from the commutator of horizontal vectors. It can be used to compute the curvatures in the state space without even knowing its metric.

### 5.4 Submersion for 1 qubit

For illustrative purposes, let us apply the method of submersion to the 1 qubit case. In order to generate a state specified by the  $(\theta, \phi)$  angles on the Bloch sphere starting from  $|0\rangle$ , we can use the following unitary

$$U_\theta = \exp \left[ \frac{i\theta}{2} (\sigma_x \cos \phi + \sigma_y \sin \phi) \right]. \quad (5.23)$$

The action of unbroken generators can be parametrized by  $V_\lambda$

$$V_\lambda = \exp \left( i \frac{\sigma_z}{2} \lambda \right), \quad (5.24)$$

and the generic  $SU(2)$  transformation is

$$U = U_\theta V_\lambda = \begin{pmatrix} e^{\frac{i\lambda}{2}} \cos\left(\frac{\theta}{2}\right) & i \sin\left(\frac{\theta}{2}\right) e^{-\frac{1}{2}i(\lambda+2\phi)} \\ i \sin\left(\frac{\theta}{2}\right) e^{\frac{1}{2}i(\lambda+2\phi)} & e^{-\frac{i\lambda}{2}} \cos\left(\frac{\theta}{2}\right) \end{pmatrix}. \quad (5.25)$$

The submersion is realised by the projection

$$\pi : (\lambda, \theta, \phi) \rightarrow (\theta, \phi), \quad (5.26)$$

and the vertical space is spanned by  $\partial_\lambda$ .

The metric on the unitary space  $M$ , with penalties  $P$  and  $Q$  as in Section 3.1, is

$$ds^2 = \frac{1}{4} \left\{ (\text{Tr}[idU U^\dagger \sigma_x])^2 + Q (\text{Tr}[idU U^\dagger \sigma_y])^2 + P (\text{Tr}[idU U^\dagger \sigma_z])^2 \right\}, \quad (5.27)$$

where

$$dU = \frac{\partial U}{\partial \theta} d\theta + \frac{\partial U}{\partial \phi} d\phi + \frac{\partial U}{\partial \lambda} d\lambda. \quad (5.28)$$

Explicitly, we find

$$dU U^\dagger = \begin{pmatrix} \frac{1}{2}i((d\lambda + d\phi)\cos(\theta) - d\phi) & \frac{1}{2}e^{-i\phi}((d\lambda + d\phi)\sin(\theta) + id\theta) \\ \frac{1}{2}ie^{i\phi}(d\theta + i(d\lambda + d\phi)\sin(\theta)) & -\frac{1}{2}i((d\lambda + d\phi)\cos(\theta) - d\phi) \end{pmatrix}. \quad (5.29)$$

Using the unitary metric, we can find the horizontal vectors fields (which are defined as orthogonal to the vertical direction  $\partial_\lambda$ )

$$\begin{aligned} h_1 &= \partial_\theta - \frac{(Q-1)\sin(\theta)\sin(2\phi)}{2(P\cos^2(\theta) + \sin^2(\theta)(Q\cos^2(\phi) + \sin^2(\phi)))} \partial_\lambda, \\ h_2 &= \partial_\phi + \frac{-2P\cos^2(\theta) + 2P\cos(\theta) - \sin^2(\theta)((Q-1)\cos(2\phi) + Q+1)}{2(P\cos^2(\theta) + \sin^2(\theta)(Q\cos^2(\phi) + \sin^2(\phi)))} \partial_\lambda, \end{aligned} \quad (5.30)$$

which have the property  $\pi(h_1) = \partial_\theta$ ,  $\pi(h_2) = \partial_\phi$ .

Then we can use eq. (5.22) to find the curvature in the states space, using the results for the 1 qubit unitaries in 3.1. An explicit calculation gives the curvature in the states space:

$$R = \frac{\alpha}{\beta}, \quad (5.31)$$

where

$$\begin{aligned} \alpha &= 8(-2(Q-1)\sin^2(\theta)\cos^2(\phi)(-P^2 + (P-1)\cos^2(\theta)(P-Q)^2 + P + Q^2) + \\ &\quad (P-1)\cos^2(\theta)(-2(P^2 - Q^2 + Q) - (P-1)(Q-1)\cos^2(\theta)(P-Q)) + P^2 \\ &\quad + (P-1)(Q-1)^2\sin^4(\theta)(P-Q)\cos^4(\phi) + P(Q-1) + (Q-1)Q), \\ \beta &= PQ((P-1)\cos^2(\theta) + (Q-1)\sin^2(\theta)\cos^2(\phi) + 1)^2, \end{aligned}$$

which matches with the one that can be calculated directly from the states metric in [52]. The difference of the sectional curvatures between the unitary and the state spaces matches with O'Neill formula

$$\Delta K = K_S(\tilde{h}_1, \tilde{h}_2) - K(h_1, h_2) = \frac{3}{4} \frac{|\mathcal{V}([h_1, h_2])|^2}{|h_1|^2|h_2|^2 - \langle h_1, h_2 \rangle^2}. \quad (5.32)$$

The plot of  $K_S(\tilde{h}_1, \tilde{h}_2)$ ,  $K(h_1, h_2)$  and  $\Delta K$  for a particular choice of penalties is shown in Fig. 4.

## 5.5 Qutrits

In this section we show an application of the method in 5.2 to determine the metric and the curvature properties in the space of states, using the explicit decomposition of the unitary space as a submersion. We consider the case of a qudit theory, which describes an atom with  $n$  energy levels. In particular, we focus on the case of qutrits, where  $n = 3$  and the group manifold is  $G = \text{SU}(3)$ .

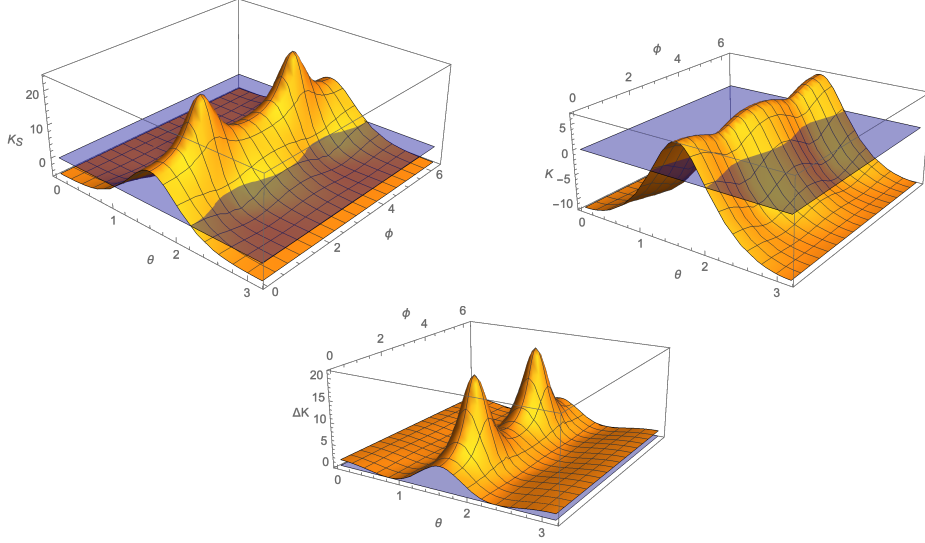


Figure 4: Comparison of  $K_S(\tilde{h}_1, \tilde{h}_2)$ ,  $K(h_1, h_2)$  and  $\Delta K$  as a function of  $(\theta, \phi)$ . The numerical values  $P = 6$ ,  $Q = 3$  have been used for illustrative purposes.

The corresponding space of states is  $G/H = \mathbb{CP}^2$ , which is parametrized by two complex coordinates  $(z_i, \bar{z}_i)$  with  $i \in \{1, 2\}$ . Alternatively, we can use four real coordinates  $(\theta_i, \phi_i)$  where  $\theta_i \in [0, \pi]$  and  $\phi_i \in [0, 2\pi]$  with  $i \in \{1, 2\}$ . The parametrization with complex coordinates is useful to transform the reference state, which we conventionally take to be  $|\psi_0\rangle = (1, 0, 0)$ , into the generic state

$$|\psi\rangle = \frac{1}{\sqrt{1 + z_i \bar{z}^i}} \begin{pmatrix} 1 \\ z_1 \\ z_2 \end{pmatrix} = \begin{pmatrix} \cos \theta_1 \\ e^{i\phi_1} \sin \theta_1 \cos \theta_2 \\ e^{i\phi_2} \sin \theta_1 \sin \theta_2 \end{pmatrix}. \quad (5.33)$$

The parametrization with angular coordinates, which we use in the second equality, will be convenient to describe the curvatures, giving a compact expression for the Ricci scalar.

The generic element of the coset<sup>2</sup> space  $G/H$  is given by

$$\begin{aligned} U_\theta^{(3)} &= \frac{1}{\sqrt{1 + z_i \bar{z}^i}} \begin{pmatrix} 1 & -\bar{z}_j \\ z_i & \sqrt{1 + z_i \bar{z}^i} \delta_{ij} - \frac{z_i \bar{z}_j}{1 + \sqrt{1 + z_i \bar{z}^i}} \end{pmatrix} = \\ &= \begin{pmatrix} \cos \theta_1 & -e^{-i\phi_1} \sin \theta_1 \cos \theta_2 & -e^{-i\phi_2} \sin \theta_1 \sin \theta_2 \\ -e^{i\phi_1} \sin \theta_1 \cos \theta_2 & \cos\left(\frac{\theta_1^2}{2}\right) - \cos(2\theta_2) \sin\left(\frac{\theta_1^2}{2}\right) & -e^{i(\phi_1 - \phi_2)} \sin\left(\frac{\theta_1^2}{2}\right) \sin(2\theta_2) \\ -e^{i\phi_2} \sin \theta_1 \sin \theta_2 & -e^{-i(\phi_1 - \phi_2)} \sin\left(\frac{\theta_1^2}{2}\right) \sin(2\theta_2) & \cos\left(\frac{\theta_1^2}{2}\right) + \cos(2\theta_2) \sin\left(\frac{\theta_1^2}{2}\right) \end{pmatrix}. \end{aligned} \quad (5.34)$$

While the last equality is specific of this case, the expression in the first line applies to the space  $\mathbb{CP}^K$  with  $K \in \mathbb{N}$  arbitrary. In the general case, the only difference is that the index runs over  $i \in \{1, \dots, K\}$ .

The group  $SU(3)$  contains as maximal subgroup  $SU(2) \times U(1)$ . In order to build the stabilizer of the element  $(1, 0, 0)$  inside  $SU(3)$ , we use a recursive procedure. The  $SU(2)$  factor corresponds to the case of a single qubit: then the stabilizer of the element  $(1, 0)$  is

<sup>2</sup>Here and in the following, the subscript refers to the coordinate dependence of the group element from the space of states ( $\theta$  subscript) or from the additional coordinates that bring to the space of unitaries ( $\lambda$  subscript). Instead the superscript ( $K$ ) refers to the group  $SU(K)$  to which the element belongs.

given by the exponential of the Pauli matrix  $\sigma_z$ , which reads

$$V_\lambda^{(2)} = e^{i\lambda_2 \sigma_z} = \begin{pmatrix} e^{i\lambda_2} & 0 \\ 0 & e^{-i\lambda_2} \end{pmatrix}. \quad (5.35)$$

Now we take the coset element of  $SU(2)$ , that can be easily taken from the lower-dimensional generalization of eq. (5.34) and reads

$$U_\lambda^{(2)} = \begin{pmatrix} \cos \lambda_1 & -e^{-i\lambda_3} \sin \lambda_1 \\ e^{i\lambda_3} \sin \lambda_1 & \cos \lambda_1 \end{pmatrix}. \quad (5.36)$$

In this way we build the generic element of  $SU(2)$  as

$$U^{(2)} = U_\lambda^{(2)} V_\lambda^{(2)} = \begin{pmatrix} e^{i\lambda_2} \cos \lambda_1 & -e^{-i(\lambda_2+\lambda_3)} \sin \lambda_1 \\ e^{i(\lambda_2+\lambda_3)} \sin \lambda_1 & e^{-i\lambda_2} \cos \lambda_1 \end{pmatrix}. \quad (5.37)$$

Finally, the stabilizer of the reference state inside  $SU(3)$  requires another  $U(1)$  factor, coming from a global phase that does not change the physics of the system. Indeed, we have the freedom to add another real variable, and the generic element of the maximal subgroup can be written as

$$V_\lambda^{(3)} = p_2 U_E^{(2)}, \quad (5.38)$$

with the phases given by the matrix

$$p_K = \begin{pmatrix} e^{iK\lambda_{2K}} & 0 & \dots & 0 \\ 0 & e^{-i\lambda_{2K}} & \dots & \dots \\ \dots & \dots & \dots & 0 \\ 0 & \dots & 0 & e^{-i\lambda_{2K}} \end{pmatrix}, \quad (5.39)$$

and where we need to embed the matrix  $U^{(2)}$  inside  $SU(3)$  as follows:

$$U_E^{(2)} \equiv \begin{pmatrix} 1 & 0 \\ 0 & U^{(2)} \end{pmatrix}. \quad (5.40)$$

In this way we finally obtain the stabilizer of the reference state as

$$V_\lambda^{(3)} = \begin{pmatrix} e^{2i\lambda_4} & 0 & 0 \\ 0 & e^{i(\lambda_2-\lambda_4)} \cos \lambda_1 & -e^{-i(\lambda_2+\lambda_3+\lambda_4)} \sin \lambda_1 \\ 0 & e^{i(\lambda_2+\lambda_3-\lambda_4)} \sin \lambda_1 & e^{-i(\lambda_2+\lambda_4)} \cos \lambda_1 \end{pmatrix}. \quad (5.41)$$

It depends on four real coordinates  $\lambda_i$ , with  $i \in \{1, 2, 3, 4\}$ .

Now we want to apply eq. (5.20) to determine the metric on the states space starting from the right-invariant form  $u_s$  and the left-invariant form  $v_s$  defined in (5.17). In addition, we need to specify the penalty matrix  $M$ . The most relevant case corresponds to penalizing the unbroken generators, because it is a configuration that allows for the existence of commutators of the form

$$[\text{easy}, \text{easy}] = \text{hard}, \quad (5.42)$$

which are expected to generate negative curvature. This happens due to the algebraic relations (3.14), which occur because we selected a maximal subalgebra. In addition, by considering  $0 \leq P < 1$ , we can also realize a relation of the form (3.12), where only the broken generators are penalized.

For these reasons, we take the penalty matrix to be

$$M = \text{diag}(P, P, P, P, 1, 1, 1, 1), \quad (5.43)$$

where the first four components refer to directions along the maximal subgroup  $SU(2) \times U(1)$ , and the last four directions to the broken generators.

We analytically compute the metric on states (5.20). The result is

$$ds_S^2 = d\theta_1^2 + \frac{2P \sin^2 \theta_1}{A(\theta_1)} d\theta_2^2 + \frac{2P \sin^2 \theta_1 \cos^2 \theta_2}{A(\theta_1)} d\phi_1^2 + \frac{C(\theta_1, \theta_2)}{A(\theta_1)B(\theta_1)} d\phi_2^2 \\ + \frac{2P \sin^2 \theta_1 \cos^2 \theta_2}{A(\theta_1)B(\theta_1)} D(\theta_1) (\cos^2 \theta_2 (d\phi_1 - d\phi_2)^2 + 2d\phi_1 d\phi_2), \quad (5.44)$$

where we defined the convenient quantities

$$A(\theta_1) \equiv (P-1) \cos(2\theta_1) + P + 1, \quad B(\theta_1) \equiv (P-1) \cos(4\theta_1) + P + 1, \quad (5.45)$$

$$C(\theta_1, \theta_2) \equiv P \sin^2 \theta_1 [B(\theta_1) - \cos(2\theta_2) (2P \cos(2\theta_1) + (P-1) \sin^2(2\theta_1))], \quad (5.46)$$

$$D(\theta_1) \equiv 3(P-1) \cos(2\theta_1) + P + 3. \quad (5.47)$$

The metric depends only on the angles  $\theta_i$  but not on the phases  $\phi_i$ . The scalar curvature reads

$$R = \frac{15}{2} \left( \frac{1}{P} - 1 \right) + \frac{14P}{((P-1) \cos^2 \theta_1 + 1)^2} + \frac{2 - 2P(3P+14)}{(P+3)(P-1) \cos^2 \theta_1 + P+3} \\ + \frac{96P}{((P-1) \cos(4\theta_1) + P+1)^2} + \frac{-8(P-1)(9P+19) \cos^2 \theta_1 + 3P(P-18) + 3}{(P+3)((P-1) \cos(4\theta_1) + P+1)}. \quad (5.48)$$

We observe that the Ricci scalar depends only on the angular coordinate  $\theta_1$ , giving a further simplification with respect to the metric on  $\mathbb{CP}^2$ . This is due to the many symmetries of the penalties in eq. (5.43).

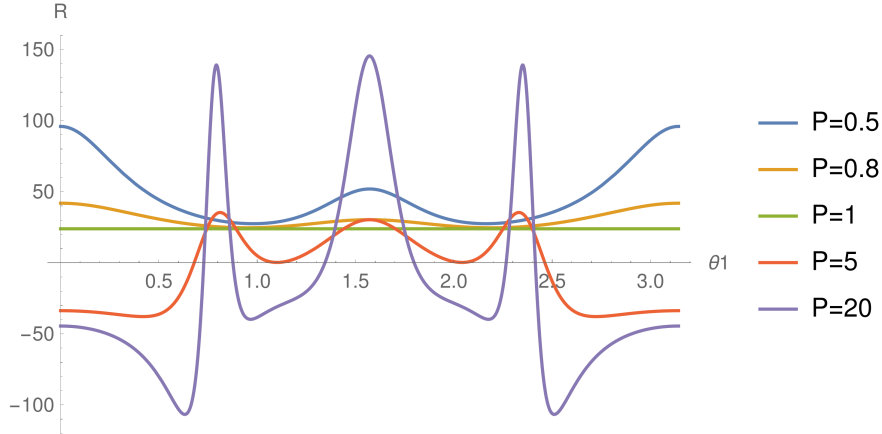


Figure 5: Scalar curvature (5.48) for the unitary space  $SU(3)$  with penalty factors  $P$  applied to all the generators of the maximal subgroup.

In Fig. 5 we plot the Ricci scalar as a function of  $\theta_1$  for different values of the penalty  $P$ . We observe that when  $0 < P < 1$  the scalar curvature is always positive, and reaches a constant value  $R = 24$  when  $P = 1$ , the case of undeformed inner product on  $SU(3)$ . When  $P > 1$  there is always a region with negative curvature which increases its size accordingly to the increasing of the penalty.

We consider the limit when  $P \rightarrow \infty$ , which means that the motion along the subgroup directions is strongly penalised. In this limit the Ricci scalar is

$$\lim_{P \rightarrow \infty} R = -\frac{3}{2} [\sec(2\theta_1)(11\sec(2\theta_1) + 12) + 4\sec^2 \theta_1 + 5]. \quad (5.49)$$

As can be seen in Fig. 6, in such a case the Ricci scalar is always negative and contains singularities. In the opposite limit  $P \rightarrow 0$  we instead obtain everywhere a positive and divergent Ricci scalar, since it contains a singular term proportional to  $P^{-1}$ .

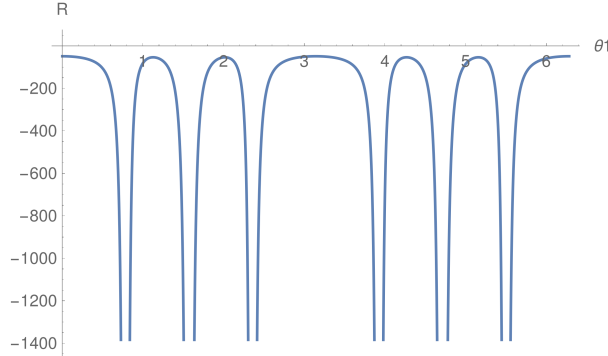


Figure 6: Scalar curvature (5.49) for the unitary space  $SU(3)$  in the limiting case of penalty  $P \rightarrow \infty$  applied to all the generators of the maximal subgroup.

The behaviour of the curvature in this example is similar to the one qubit case with  $Q = 1$  and  $P$  generic, which was studied in detail in [52].

## 5.6 Submersions and geodesics

The relation between geodesics in  $B$  and geodesics in  $M$  for generic submersions was studied in [54]. An important result is that, if a geodesic in  $M$  is horizontal at some point, it remains horizontal. Then the projection by  $\pi$  of an horizontal geodesic is a geodesic in the space of states  $B$ . As a general result, we have that for submersions from complete manifolds  $M$  as our unitary space, every geodesic of  $B$  can be built as the projection of a horizontal geodesic in  $M$ . It is important to stress that the projection of a geodesic which is not horizontal in general does not provide a geodesic on  $B$ .

We know from eq. (2.9) that the exponential of an eigenvector of the penalty matrix  $\mathcal{G}$  is a geodesic in the unitary space. Combining with the previous result, the exponential of an eigenstate of  $\mathcal{G}$  which is also perpendicular to the unbroken subgroup at the origin, gives a geodesic in the state space  $B$ . This property provides us a simple class of geodesics in some particular situations. In the 1-qubit case, this is studied in Section 6.3.

Let us instead consider the 2-qubits case with penalties depending just on the weights. Taking as reference state  $|00\rangle$ , the unbroken subgroup is generated by the following generators:

$$\begin{aligned} & \mathbb{1} \otimes \sigma_z, \quad \sigma_z \otimes \mathbb{1}, \quad \sigma_z \otimes \sigma_z, \\ & \sigma_x \otimes (\mathbb{1} - \sigma_z), \quad \sigma_y \otimes (\mathbb{1} - \sigma_z), \quad (\mathbb{1} - \sigma_z) \otimes \sigma_x, \quad (\mathbb{1} - \sigma_z) \otimes \sigma_y, \\ & \sigma_x \otimes \sigma_y - \sigma_y \otimes \sigma_x, \quad \sigma_x \otimes \sigma_x + \sigma_y \otimes \sigma_y. \end{aligned} \quad (5.50)$$

The orthogonal complement to this space is generated by:

$$\begin{aligned} & \sigma_x \otimes (\mathbb{1} + \alpha \sigma_z), \quad \sigma_y \otimes (\mathbb{1} + \alpha \sigma_z), \quad (\mathbb{1} + \alpha \sigma_z) \otimes \sigma_x, \quad (\mathbb{1} + \alpha \sigma_z) \otimes \sigma_y, \\ & S_2^- = \sigma_x \otimes \sigma_y + \sigma_y \otimes \sigma_x, \quad S_2^+ = \sigma_x \otimes \sigma_x - \sigma_y \otimes \sigma_y, \end{aligned} \quad (5.51)$$

where  $\alpha$  is a coefficient<sup>3</sup> dependent from the penalty factors, chosen to ensure orthogonality with unbroken generators in eq. (5.50). Note that just the last two generators  $S_2^\pm$  in eq.

<sup>3</sup>The precise value is completely irrelevant for the following discussion.

(5.51) have a definite weight  $w = 2$ , and so just these two operators generate exponential horizontal geodesics.

We can generalise this arguments to  $n$  qubits as follows. Let us take as a reference state  $|00 \dots 0\rangle$ . Let us consider the action of a infinitesimal transformation on this state, with  $w = n$  and which contains just  $\sigma_x$  and  $\sigma_y$  entries in the tensor product. This operator will rotate the state as

$$|00 \dots 0\rangle \rightarrow |00 \dots 0\rangle + \epsilon |11 \dots 1\rangle, \quad (5.52)$$

where  $\epsilon$  is an infinitesimal complex number. This sector of operators contain  $2^n$  generators; out of this set, a vector space of dimension  $2^n - 2$  operators is unbroken. So, in the  $w = n$  sector which contain just tensor products of  $\sigma_x$  and  $\sigma_y$  we can always find a broken dimension 2 subspace which is orthogonal to the vertical space

Let us build these generators explicitly. We introduce

$$A_s^n = \frac{1}{\binom{n}{s}} \sum_{(k_1, \dots, k_n)} \sigma_{k_1} \otimes \dots \otimes \sigma_{k_n} \quad (5.53)$$

where the sum runs over all the permutation  $(k_1, \dots, k_n)$  which contain  $s$  generators  $\sigma_y$  and  $n - s$  generators  $\sigma_x$ . Then the two generators

$$S_n^+ = \sum_{0 \leq k \leq n}^{k \text{ even}} i^k A_k^n, \quad S_n^- = \sum_{0 \leq k \leq n}^{k \text{ odd}} i^{k+1} A_k^n. \quad (5.54)$$

are both broken by the reference states and orthogonal to all the unbroken  $w = n$  generalised Pauli matrices which contain just  $\sigma_x$  and  $\sigma_y$  in the tensor product. This construction generalise to  $n$  qubits the two operators in the last line of eq. (5.51).

Then we can look for other states orthogonal to the vertical space. We can consider a state of the form  $S_{n-1}^\pm \otimes (\mathbb{1} + \alpha_1 \sigma_z)$  with the coefficient chosen in such a way that is is orthogonal to  $S_{n-1}^\pm \otimes (\mathbb{1} - \sigma_z)$ . This involves a linear combination of weight  $n$  and  $n - 1$  states, and in general one can find  $2\binom{n}{1}$  such states. One can iterate the construction, looking for states of the form

$$S_{n-s}^\pm \otimes (\mathbb{1} + \alpha_s \sigma_z)^s, \quad (5.55)$$

and determine  $\alpha_s$  in such a way that the state is orthogonal to the unbroken operators

$$S_{n-s}^\pm \otimes (\mathbb{1} - \sigma_z) \otimes \mathbb{1}^b \otimes \sigma_z^c, \quad (5.56)$$

where  $b, c$  are some integers numbers. For each integer  $s$ , this states are linear combination of weights  $w$  with

$$n - s \leq w \leq n. \quad (5.57)$$

There are  $2\binom{n}{s}$  of such states, with  $1 \leq s \leq n$ . In this way one can build all the  $2^n - 1$  horizontal vectors in the unitary spaces, which project to the  $\mathbb{CP}^{2^n-1}$  directions in the state space. A broken unitary labelled by  $s$  is a linear combination of states with weight  $w$  with  $n - s \leq w \leq n$ .

If the penalties of each weight  $q_w$  are all different (as in the progressive model), just the  $s = 0$  broken unitaries  $S_n^\pm$  are penalty eigenstates. This is the most generic case. The only exponential horizontal geodesic are generated by linear combination of  $S_n^+$  and  $S_n^-$ .

If some penalties for different weights are degenerate, we can find more eigenstates of the penalties which are orthogonal to the unbroken subgroup. For example, in the draconian model all the weights with  $3 \leq w \leq n$  are the same, and so all the broken unitaries with  $0 \leq s \leq n - 3$  generate projectable exponential geodesics.

There is a relation between conjugate points in  $M$  and  $B$  [54]. Let us consider a horizontal geodesic

$$\gamma(t) : [a, b] \rightarrow M \quad (5.58)$$

and let  $\gamma(t_0)$  be the first conjugate point of  $\gamma$  along the geodesic starting from  $\gamma(a)$ . Then the projected geodesic  $\beta(t) = \pi(\gamma(t))$  has a conjugate point for  $t'_0 \leq t_0$ .

## 6 Towards an exponential complexity

The definitions of unitary and state complexity require the minimization of the length of a path connecting the identity with a generic unitary, or the reference state to the target state, respectively. In the following, we exploit the techniques developed in the previous sections to find explicit classes of geodesics and to find their conjugate points, which play an important role in the minimisation process.

### 6.1 Conjugate points and Raychaudhuri equation

An important problem in the geometric approach to complexity is to determine the minimal length geodesics that connect the identity to a given unitary. From a general result in Riemannian geometry, a geodesic does not minimise lengths anymore after its first conjugate point. This is not a necessary condition: there could be a globally shorter path before the first conjugate point.

A useful tool to study conjugate points is the Raychaudhuri equation (see e.g. [64] for a review). Let us consider a congruence of geodesics which is orthogonal to a family of hypersurfaces in an arbitrary Riemannian manifold. Let us denote by  $u^\alpha$  the tangent vector field to the geodesics, with  $u^\alpha u_\alpha = 1$ . The geodesics are in affine parameterization, i.e.  $u^\beta D_\beta u^\alpha = 0$ , where  $D_\beta$  is the covariant derivative. The deviation vectors  $\xi^\mu$  are taken orthogonal to  $u^\alpha$ , i.e.  $\xi^\alpha u_\alpha = 0$ . We can define the transverse part of the metric as:

$$h_{\alpha\beta} = g_{\alpha\beta} - u_\alpha u_\beta, \quad (6.1)$$

and the tensor

$$B_{\alpha\beta} = D_\beta u_\alpha, \quad (6.2)$$

which can be shown to be symmetric if the congruence of geodesics is orthogonal to a family of hypersurfaces. Moreover  $B_{\alpha\beta}$  can be decomposed in the trace and traceless part

$$B_{\alpha\beta} = \frac{1}{d-1} \Theta h_{\alpha\beta} + \sigma_{\alpha\beta}, \quad (6.3)$$

where  $d$  is the dimension of space,  $\Theta$  is the expansion scalar and  $\sigma_{\mu\nu}$  the (traceless and symmetric) shear tensor. The expansion scalar  $\Theta$  measures the time derivative of a transverse volume of the geodesic, i.e.

$$\Theta = \frac{1}{\Delta V} \frac{d\Delta V}{d\lambda} \quad (6.4)$$

where  $\Delta V$  is an infinitesimal transverse volume.

If the scalar  $\Theta$  approaches  $-\infty$  in some point  $r$  along a geodesic, it detects the presence of conjugate points for our congruence of geodesics. This means that the geodesic that we are studying does not anymore give us the minimal distance for points beyond  $r$ . The Raychaudhuri equation determines the evolution of  $\Theta$  along the geodesic flow:

$$\frac{d\Theta}{d\lambda} = -\frac{1}{d-1} \Theta^2 - \sigma^{\alpha\beta} \sigma_{\alpha\beta} - R_{\alpha\beta} u^\alpha u^\beta, \quad (6.5)$$

where  $R_{\alpha\beta}$  is the Ricci tensor and  $\lambda$  is an affine parameter. There exists also an equation for the traceless part  $\sigma_{\alpha\beta}$ , see e.g. [65], which in Euclidean signature is:

$$\frac{D\sigma_{\mu\nu}}{d\lambda} = -\frac{2}{d-1}\Theta\sigma_{\mu\nu} - \sigma_{\mu}^{\sigma}\sigma_{\nu\sigma} + \frac{1}{d-1}h_{\mu\nu}\sigma^{\alpha\beta}\sigma_{\alpha\beta} - C_{\mu\alpha\nu\beta}u^{\alpha}u^{\beta} - \frac{1}{d-2}\bar{R}_{\mu\nu}, \quad (6.6)$$

where

$$\bar{R}_{\mu\nu} = h_{\mu}^{\alpha}h_{\nu}^{\beta}R_{\alpha\beta} - \frac{1}{(d-1)}R_{\alpha\beta}h^{\alpha\beta}h_{\mu\nu}, \quad (6.7)$$

it the projected trace-free part of  $R_{\mu\nu}$ .

## 6.2 An application to a simple class of geodesics

From eq. (2.9), we know that in the unitary space the exponential of an eigenvector of the penalty factor matrix  $\mathcal{G}$  gives us a geodesic. It is particularly convenient to apply the Raychaudhuri equation to this class of geodesics, which have constant  $R_{\alpha\beta}u^{\alpha}u^{\beta}$ . If we neglect the term  $\sigma^{\alpha\beta}\sigma_{\alpha\beta}$  in eq. (6.5), the equation can be solved analytically. In general this term is non-zero (see appendix A), but it is positive definite. So, neglecting the  $\sigma^{\alpha\beta}\sigma_{\alpha\beta}$  term gives us an upper bound for the presence of a conjugate point along a geodesic.

Let us first solve it in the limit  $\Theta \rightarrow \infty$ , as it is the case for a family of geodesics starting from the same point. In this case we can neglect  $R_{\alpha\beta}u^{\alpha}u^{\beta}$ , leading to:

$$\dot{\Theta} + \frac{1}{d-1}\Theta^2 = 0, \quad \Theta = \frac{d-1}{\lambda-k}, \quad (6.8)$$

$k$  is an integration constant. This approximation is the same as considering the flat space limit. In order to consider a family of geodesics which start at the same point at  $\lambda = 0$ , we set  $k = 0$ . Let us now consider

$$\dot{\Theta} + \frac{1}{d-1}\Theta^2 + B = 0, \quad (6.9)$$

where  $B = R_{\alpha\beta}u^{\alpha}u^{\beta}$ . The conjugate point, in this approximation, shows up only for  $B > 0$ . Requiring that at small  $\lambda$  the solution reproduces the flat space one  $\Theta = (d-1)/\lambda$ , we find:

$$\Theta = \sqrt{B(d-1)} \cot\left(\sqrt{\frac{B}{d-1}}\lambda\right), \quad (6.10)$$

and so it has a conjugate at

$$\lambda_0 = \frac{\pi\sqrt{d-1}}{\sqrt{B}}. \quad (6.11)$$

Since  $\sigma^{\alpha\beta}\sigma_{\alpha\beta}$  is a positive-definite quantity, the value of  $\lambda_0$  provides an upper bound for the distance  $\lambda_c$  of the conjugate point from the origin:

$$\lambda_c \leq \lambda_0 = \frac{\pi\sqrt{d-1}}{\sqrt{R_{\alpha\beta}u^{\alpha}u^{\beta}}}. \quad (6.12)$$

Note that, keeping the Ricci curvature fixed,  $\lambda_0$  scales exponentially with the number of qubits due to the factor  $\sqrt{d-1} \approx 2^n$ . This is a first evidence of the exponential nature of the maximal complexity.

### 6.3 One qubit

In order to make the discussion concrete with a clear example we will consider the one qubit case, see Section 3.1. In this case the unitaries manifold is a generalised Berger sphere and an explicit expression for the metric is available. Introducing the coordinates  $(\theta_x, \theta_y, \theta_z)$  to parameterize the unitary

$$U = e^{i\sigma_z\theta_z} e^{i\sigma_y\theta_y} e^{i\sigma_x\theta_x}, \quad (6.13)$$

the metric can be written explicitly:

$$g_{ij} = \frac{1}{2} \begin{pmatrix} \Xi & (1-Q) \cos 2\theta_y \sin 4\theta_z & 2P \sin 2\theta_y \\ (1-Q) \cos 2\theta_y \sin 4\theta_z & (Q-1) \cos 4\theta_z + Q + 1 & 0 \\ 2P \sin 2\theta_y & 0 & 2P \end{pmatrix}, \quad (6.14)$$

where

$$\Xi = 2(P \sin^2 2\theta_y + \cos^2 2\theta_y (Q \sin^2 2\theta_z + \cos^2 2\theta_z)). \quad (6.15)$$

We know from the general analysis that the exponentials of  $\sigma_x, \sigma_y, \sigma_z$  are geodesics, with

$$\begin{aligned} G_x : \quad & \theta_x = \lambda, \quad \theta_y = \theta_z = 0, \\ G_y : \quad & \theta_y = \frac{\lambda}{\sqrt{Q}}, \quad \theta_x = \theta_z = 0, \\ G_z : \quad & \theta_z = \frac{\lambda}{\sqrt{P}}, \quad \theta_x = \theta_y = 0; \end{aligned} \quad (6.16)$$

as can be also checked directly from the geodesic equations of the metric (6.14).

We have seen that the presence of conjugate points on this simple class of geodesics can be detected by the Ricci tensor:

$$\begin{aligned} R_x &= \frac{2(1 - (P - Q)^2)}{PQ}, & R_y &= \frac{2(Q + P - 1)(Q - P + 1)}{PQ}, \\ R_z &= \frac{2(P + Q - 1)(P - Q + 1)}{PQ}, \end{aligned} \quad (6.17)$$

where we denote  $R_{x,y,z} \equiv R_{\sigma_x, \sigma_y, \sigma_z}$ .

Conjugate points of the geodesic  $G_k$  in eq. (6.16) occur in the regions of the parameter space  $(P, Q)$  where the corresponding  $R_k$  is positive, see Fig. 7. In particular, each of the geodesics  $G_k$  for  $k = x, y, z$  develops a conjugate point in the region where  $R_k > 0$  for

$$\lambda_c \leq \lambda_0, \quad \lambda_0 = \frac{\pi\sqrt{2}}{\sqrt{R_k}}. \quad (6.18)$$

A plot of an example of conjugate point is shown in Figure 7 in stereographic projection.

Using eq. (6.6), it is also possible to include the  $\sigma^{\alpha\beta}\sigma_{\alpha\beta}$  corrections, in order to determine in general the exact location of the conjugate points. Using eq. (6.6), we can show that  $\sigma^{\alpha\beta}$  vanishes for  $G_x$  in the  $P = Q$  case. It also vanishes for  $G_y$  in the  $P = 1$  case and for  $G_z$  in the  $Q = 1$  case (see Appendix A). We have then a few exact results:

- For  $Q = 1$ ,  $G_z$  has a conjugate point at  $\lambda = \frac{\pi}{\sqrt{P}}$
- For  $P = 1$ ,  $G_y$  has a conjugate point at  $\lambda = \frac{\pi}{\sqrt{Q}}$
- For  $P = Q$ ,  $G_x$  has a conjugate point at  $\lambda = \pi P$ .

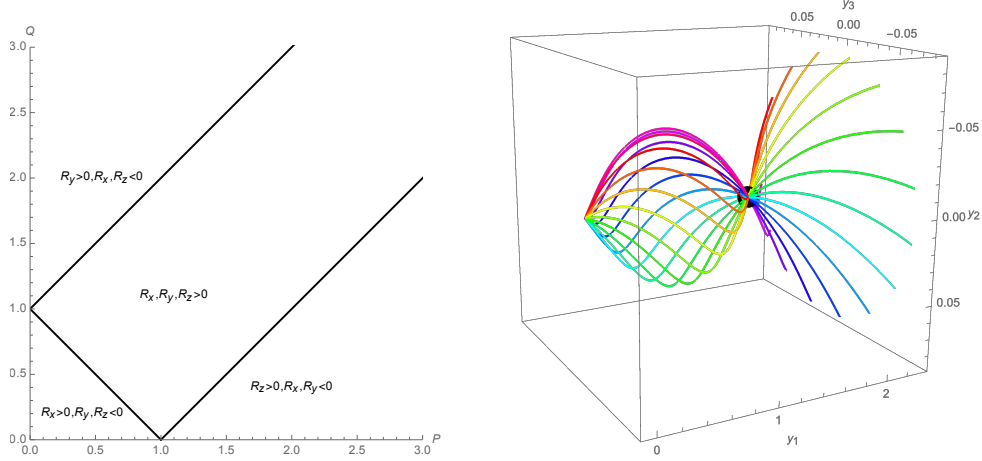


Figure 7: Left: Regions where each  $R_{x,y,z}$  is positive. Right: Example of a conjugate point of geodesics for  $P = Q = 0.4$  in stereographic projection.

In particular, it is interesting to consider the limit in eq. (3.3), with  $P = 1$  and  $Q \rightarrow \infty$ . In this case the only exponential geodesic with a conjugate point is  $G_y$ . In the limit  $Q \rightarrow \infty$  the conjugate point moves very close to the origin, at  $\theta_y = \pi/Q$  and at  $\lambda = \pi/\sqrt{Q}$ . The  $G_y$  geodesic is then minimising only very close to the origin, and the limit is singular. Indeed we already expected a singularity from the behaviour of curvatures, see eq. (3.4). Also, sending the penalty  $Q$  to infinity does not correspond to getting a big complexity in the  $\sigma_y$  direction: a shortcut with length scaling as  $1/\sqrt{Q}$  is for sure available just after the conjugate point. This is an indication of low maximal complexity and it is correlated to a singular limit in the curvature.

It is also interesting to consider the limit in eq. (3.5), where  $P = Q \rightarrow \infty$ . The Ricci curvatures are all positive:

$$R_x = \frac{2}{P^2}, \quad R_y = R_z = \frac{4}{P} - \frac{2}{P^2}. \quad (6.19)$$

In this case  $G_x$  has an exact conjugate point at  $\theta_x = \lambda = \pi P$ , while  $G_{y,z}$  have conjugate points for  $\lambda \lesssim \pi\sqrt{P/2}$ , which correspond to  $\theta_y, \theta_z$  of order 1. There is no singularity in geodesic, as expected from the curvatures in (3.6). Note that, while the distance of the conjugate point in  $G_{y,z}$  diverges, their position in the coordinate  $\theta_{y,z}$  approaches a finite limit for  $P \rightarrow \infty$ . The limit of large penalty indeed may correspond to a large maximal complexity, because no obvious shortcuts are available. This is supported by numerical computations: the points with large complexity lay nearby the conjugate point, and so the maximal complexity scales as  $\sqrt{P}$ .

In the one qubit case, the exponential geodesics on unitary space can be projected to the states space using the submersion, as explained in Section 5.6. Taking as a reference state  $|0\rangle$ , the unbroken subgroup is generated by  $\sigma_z$ . The geodesics shooted in the orthogonal directions  $\sigma_x$  and  $\sigma_y$  are then horizontal and projectable. For generic  $P, Q$  there are then two exponential horizontal geodesics. The corresponding geodesics on states can be obtained by the projection of these curves by the submersion  $\pi$ .

It is more intuitive to plot the geodesics in the states space, since it is a 2-dimensional space. In the one qubit case, the metric for states in the standard Bloch sphere coordinates  $(\theta, \phi)$  is

$$g_{ij} = \frac{1}{\Psi} \begin{pmatrix} \Lambda & P(Q-1)\sin(\theta)\cos(\theta)\sin(\phi)\cos(\phi) \\ P(Q-1)\sin(\theta)\cos(\theta)\sin(\phi)\cos(\phi) & P\sin^2(\theta)(Q\cos^2(\phi) + \sin^2(\phi)) \end{pmatrix} \quad (6.20)$$

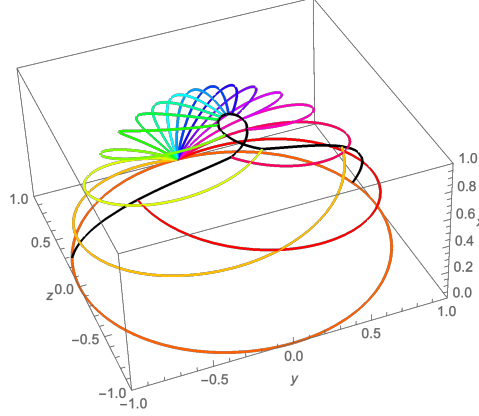


Figure 8: Geodesics with length  $\lambda = 2.5$  for  $Q = 10$ ,  $P = 10$ . The geodesics are plotted in different colours. The endpoints of the various curves are represented in black.

where

$$\begin{aligned}\Lambda &= P \cos^2(\theta) \cos^2(\phi) + PQ \cos^2(\theta) \sin^2(\phi) + Q \sin^2(\theta), \\ \Psi &= 4 \{ \sin^2(\theta) \sin^2(\phi) + P \cos^2(\theta) + Q \sin^2(\theta) \cos^2(\phi) \} .\end{aligned}\quad (6.21)$$

We checked numerically that the projection of the horizontal geodesics in the unitary space corresponds to geodesics in the states space, as is required by general results on submersions.

It is then interesting to plot the geodesics for the case of large  $P$  and  $Q$  in the state space. In Fig. 8 are shown the geodesics for the case  $P = Q = 10$  on the Bloch sphere. In particular we see that the maximal complexity region lies just before the conjugate point in  $\sigma_y$ . Such a point lies inside the *drop* delimited by the self intersection of the black curve. As it is clear from the figure no geodesics of length less than  $\lambda$  can penetrate inside the drop.

#### 6.4 Draconian model

In order to study conjugate points in the draconian model we can use the results from [5] for  $R_\sigma$ , where  $\sigma$  is a generalised Pauli matrix with weight  $w$ :

$$\begin{aligned}w &= 1, & R_\sigma &= 2(3n - 2) + \frac{1}{q^2} \left( \frac{4^n}{2} - 2(3n - 2) \right), \\ w &= 2, & R_\sigma &= -24q(n - 2) + 8(6n - 11) + \frac{1}{q^2} \left( \frac{4^n}{2} - 8(3n - 5) \right), \\ w &= 3, & R_\sigma &= \frac{1}{q} \left( 12q^2 + \frac{4^n}{2} + 36(n - 3) - \frac{1}{q} 12(3n - 8) \right), \\ w &\geq 4, & R_\sigma &= \frac{1}{q} \left( \frac{4^n}{2} + 4w(3n - 2w) - \frac{1}{q} 4w(3n - 2w) \right).\end{aligned}\quad (6.22)$$

These expressions are valid for arbitrary  $n$  and  $q$ . In particular, for  $q = 1$ , we recover the cases with uniform penalties  $q(w) = 1$ , where all the  $R_\sigma$  are the same, i.e.  $R_\sigma = 4^n/2$ . In order to have negative scalar curvature, we have to scale  $q$  with  $n$  as  $q \approx \mathcal{O}(4^n)$ .

In studying conjugate points along the exponential geodesics, it is interesting to consider not only the distance  $\lambda$  from the origin, but also their position in a coordinate  $\theta$ , which

runs along the geodesic and does not scale with the penalty. We can define  $\theta$  as the length of the exponential geodesic in the case with all the penalties  $q_\sigma = 1$  (bi-invariant metric).

We can use eq. (6.12) with  $d = 4^n - 1$  to get an estimate of the distance of conjugate points from origin:

$$\begin{aligned} w &= 1, & \lambda_0 &\approx \frac{\pi 2^n}{\sqrt{6n}}, & \theta_0 &= \lambda_0, \\ w &= 3, & \lambda_0 &\approx \frac{\pi 2^n}{\sqrt{12q}} \approx \frac{\pi}{\sqrt{12}}, & \theta_0 &= \frac{\lambda_0}{\sqrt{q}} \approx \frac{1}{2^n} \frac{\pi}{\sqrt{12}}, \\ w &\geq 4, & \lambda_0 &\approx \pi \sqrt{2q} \approx \sqrt{2\pi} 2^n, & \theta_0 &= \frac{\lambda_0}{\sqrt{q}} \approx \sqrt{2\pi}, \end{aligned} \quad (6.23)$$

where we have inserted  $q \approx 4^n$  (in order to have negative scalar curvature) and  $\theta_0$  is the length of this geodesic in the unpenalised metric  $q_\sigma = 1$ .

The geodesics with  $w = 1$  have a conjugate point after a length which is exponential in  $n$ , but this does not correspond to a cut locus, because this is achieved for an angle  $\theta$  which is also exponential in  $n$ . This corresponds to winding around the Hilbert space several times.

The geodesics with  $w \geq 4$  instead have a conjugate point at  $\theta$  of order 1, with a length which scales exponentially in  $n$ . If in addition we would know that the cut locus coincides with the conjugate point, this would be a proof that maximal complexity is scaling exponentially with  $n$ . Unfortunately, we don't have a strong indication that this happens. Still, the fact that  $\theta$  remains of order 1 makes the possibility that the cut locus coincides with conjugate point not as unrealistic as in the  $w = 1$  case. Note that, with very good approximation, there is no dependence on  $w$  for  $w \geq 4$  in the distance of the conjugate point from the origin.

The geodesics with  $w = 3$  have a conjugate point at a value of the coordinate  $\theta$  very close to the identity. In this limit we have evidence that the conjugate point is also a cut locus, because it happens at infinitesimal value of the coordinate  $\theta$ . However, the distance from the origin is of order 1, so this does not teach us anything interesting about the possible exponential growth of complexity at large  $n$ . Also, the exponential dependence  $\theta \propto 2^{-n}$  shows that draconian penalties are by construction singular.

From the results in Section 5.6, we know that we can find many directions orthogonal to the unbroken subgroup which are also penalties eigenvectors. In particular, all the tangent directions orthogonal to the vertical space with  $0 \leq s \leq n - 3$ , see eq. (5.57), contain just operators with weight  $w \geq 3$  and so generate exponential projectable geodesics. The considerations about conjugate points for these exponential geodesics can then be extended to the state space, with the caveat that the conjugate point might occur before in the state space, see [54].

## 6.5 Progressive model

At leading order in  $\alpha$ , the Ricci contraction with the unit vector pointing in the direction  $\sigma$  is (for  $w > 1$ )

$$R_w = 2w (2^{w-1} - 2^{2n-2w+1}), \quad (6.24)$$

and  $R_w = 2$  for  $w = 1$ . This is positive for  $w = 1$  and for

$$w > \frac{2}{3}(n+1). \quad (6.25)$$

The conjugate point for  $w = 1$  is estimated at

$$\lambda_0 = \theta_0 = \frac{\pi}{\sqrt{2}} 2^n, \quad (6.26)$$

and does not correspond to a point where a geodesic ceases to be minimising. This is because it is along the easiest direction with  $\lambda = \theta$ , and so it happens after that the geodesic has crossed the Hilbert space of states many times.

The conjugate points for the generators at large  $w$  in eq. (6.25) are more interesting. In this class, the largest positive  $R_k$  is at  $w = n$ , which gives

$$R_n = n(2^n - 4), \quad (6.27)$$

and gives a conjugate point at

$$\lambda_0 = \frac{\pi 2^{n/2}}{\sqrt{n}}, \quad \theta_0 = \frac{\lambda_0}{\alpha^{n/2}} = \frac{\pi 2^{n/2}}{\sqrt{n} \alpha^{n/2}}. \quad (6.28)$$

The smallest positive value of  $R_k$  is realised for slightly different values of the integer  $w$ , depending on the value of  $n$  modulo 3. We have to distinguish the following cases:

$$\begin{aligned} n = 3a, \quad w &= 2\frac{n}{3} + 1, \quad R_w = 2^{2n/3} \left(1 + \frac{2n}{3}\right) \approx n 2^{2n/3} 0.67, \\ n = 3a + 1, \quad w &= \frac{2n + 4}{3}, \quad R_w = 2^{2n/3} (n + 2) 2^{1/3} \approx n 2^{2n/3} 1.26, \\ n = 3a + 2, \quad w &= \frac{2n + 5}{3}, \quad R_w = 2^{2n/3} \frac{7(2n + 5)}{6 \cdot 2^{1/3}} \approx n 2^{2n/3} 1.85, \end{aligned} \quad (6.29)$$

where  $a$  is an integer number. In all cases  $R_w \approx n 2^{2n/3}$  up to order one factors. This gives a conjugate point at:

$$\lambda_0 = \frac{\pi 2^{2n/3}}{\sqrt{n}}, \quad \theta_0 = \frac{\lambda_0}{\alpha^{2n/3}} = \frac{\pi 2^{2n/3}}{\sqrt{n} \alpha^{2n/3}}. \quad (6.30)$$

Intermediate values of the weight give conjugate points which scale in between the ones in eqs (6.28) and (6.30).

In order to have small  $\theta_0$  in the large  $n$  limit in eqs. (6.28) and (6.30), we have just to require  $\alpha > 2$ . The required value of  $\alpha$  should be also large enough in order to trust the approximation eq. (6.24). The Ricci indeed seems to converge to the asymptotic value quite fast (see Fig. 2 for the Ricci scalar).

Since  $\theta_0 \rightarrow 0$ , we expect that, for large  $n$ , the geodesics in eq. (6.28) and (6.30) are truly minimising ones. So we find strong indication that in this limit the distance of the cut locus of the geodesics with large  $w$  (in the window  $\frac{2}{3}n < w < n$ ) is in between

$$\frac{\pi 2^{n/2}}{\sqrt{n}} \leq \lambda_0 \leq \frac{\pi 2^{2n/3}}{\sqrt{n}}. \quad (6.31)$$

Consequently, the maximal complexity is bigger than

$$\lambda_{\max} = \frac{\pi 2^{2n/3}}{\sqrt{n}}, \quad (6.32)$$

and scales exponentially in  $n$ .

One may wonder if this is just an artifact of the large  $\alpha$  limit: indeed in this regime we expect that the maximal complexity goes to infinity by construction. In order to clarify this subtle point, let us consider higher order corrections to  $R_w$  and to  $\lambda$ . The order  $\alpha^{-1}$  term vanishes for all the Ricci, except for  $w = 2$  which is not interesting for conjugate points. So we need to go to order  $\alpha^{-2}$ .

To make the computation simpler, let us consider  $w = n$ . In this case, the non-vanishing  $\alpha^{-2}$  terms in the sectional curvatures which contribute to  $R_n$  are:

$$\begin{aligned}\delta K(n, 2, 0) &= -\frac{3}{\alpha^2}, & \delta K(n, 3, 0) &= \frac{2}{\alpha^2}, \\ \delta K(n, n-2, 0) &= -\frac{2}{\alpha^2}, & \delta K(n, n-1, 0) &= \frac{1}{\alpha^2}, \\ \delta K(n, N, 1) &= \frac{1}{\alpha^2}, & \text{for } 4 \leq N \leq n-1.\end{aligned}\quad (6.33)$$

A direct calculation gives

$$R_n = n(2^n - 4) + \frac{(n-1)n((2^n - 16)n - 2(2^n - 4))}{6\alpha^2} \approx n \cdot 2^n + \frac{1}{6\alpha^2} n^3 2^n. \quad (6.34)$$

The length of the geodesic built from the exponential of a  $w = n$  generator before the conjugate point is then, at the next order in  $\alpha$ :

$$\lambda_0 = \frac{\pi \cdot 2^n}{\sqrt{n \cdot 2^n + \frac{n^3}{6\alpha^2} 2^n}} \approx \frac{\pi}{\sqrt{n}} 2^{n/2} \left(1 - \frac{1}{12\alpha^2} n^2\right). \quad (6.35)$$

In order to trust the approximation we should just increase  $\alpha$  in a way slightly faster than  $n$  for large  $n$ , for example quadratically. From this polynomial increase of  $\alpha$  with  $n$ , we get an exponential increase of complexity. We believe that this is a strong indication that maximal complexity scales exponentially with  $n$  with a progressive choice of penalties.

This is not a rigorous proof. For example, we neglected the shear term in Raychaudhuri equation which may cause the conjugate point to appear before it. It would be interesting to improve the analysis studying the impact of these terms. We leave this as a problem for future investigation.

From Section 5.6, we know that for the progressive model there is just a two dimensional space of vectors which are both orthogonal to the vertical space and also eigenstates of the penalty. They are generated by arbitrary linear combinations of  $S_n^\pm$  in eq. (5.54) and they have both  $w = n$ . So the previous calculation in unitary space for  $w = n$  applies also for state complexity, with the caveat that the conjugate point might occur before in the state space, see [54].

## 7 Conclusions

In this paper we studied several aspects of complexity geometry. Using the formalism introduced in [5] for a unitary complexity of a system of  $n$  qubits, we showed that the negativity of sectional curvatures  $K$  along the directions  $\rho, \sigma$  in unitary space is directly related to a large penalty factor for the commutator  $[\rho, \sigma]$ , i.e.

$$K(\rho, \sigma) = \frac{1}{q_\rho q_\sigma} \left[ -3 q_{[\rho, \sigma]} + 2(q_\rho + q_\sigma) + \frac{(q_\rho - q_\sigma)^2}{q_{[\rho, \sigma]}} \right]. \quad (7.1)$$

In this equation, the only negative term is proportional to the penalty of  $[\rho, \sigma]$ , so that in order to get a negative  $K(\rho, \sigma)$  the penalty  $q_{[\rho, \sigma]}$  has to dominate compared to  $q_\rho$  and  $q_\sigma$ ; this is always possible for large enough  $q_{[\rho, \sigma]}$ . From this expression is clear that negative curvature is always associated to commutators of the form

$$[\text{easy}, \text{easy}] = \text{hard}, \quad (7.2)$$

where easy and hard refer to small and large penalty factors. This is consistent with the analysis in [52].

We applied the formalism of [5] to various examples, both for small and large number of qubits. The one qubit is already an interesting nutshell for some generic properties (see section 3.1). First of all, one qubit is a universal closed subsector of the  $n$ -qubits space, because sectional curvatures inside each qubit space depend just on the penalties of this subsector. In the generic one qubit parameter space, we have that at least 2 out of 3 of the sectional curvatures in the orthogonal basis are positive. This argument shows that, for complexity geometry of  $n$  qubits, at least some sectional curvatures are always positive. Moreover, some of the possible behaviours that are realised when some of the penalty factors are sent to infinity generalise to large number of qubits. There are two prototypical situations:

1. if the easy generators (which are the ones whose penalties are not sent to infinity) are enough to construct the generic unitary, the maximal complexity does not diverge. Some of the sectional curvatures instead diverge and the geometry is singular. An example of this case is realised for  $Q \rightarrow \infty$  and  $P$  constant.
2. if the remaining easy generators are *not* enough to construct the generic unitary, the maximal complexity is infinity by construction and the sectional curvatures do not diverge. An example of this case is for  $P = \beta Q \rightarrow \infty$ , with  $\beta$  constant, where both vanishing (for  $\beta = 1$ ) and negative (for  $\beta \neq 1$ ) scalar curvatures can be realised.

For a larger number of qubits  $n$  the situation is much more intricate because the dimension of the Hilbert space of unitaries scales as  $4^n$ . The allowed values of sectional curvatures in the orthogonal basis have large multiplicities, which can scale exponentially or polynomially with  $n$  and the weight  $w$ . In section 4 we provide general expressions for this counting. For large  $n$  we have a huge arbitrariness in the choice of the penalty factors. Two useful prototypes are:

- draconian penalties, defined by eq. (1.1). In the large  $q$  limit, for fixed  $n$ , complexity does not diverge, and the geometry becomes singular. This is similar to point 1 of the one qubit case.
- progressive penalties, as defined in eq. (1.2). In the large  $\alpha$  limit, complexity diverges for fixed  $n$  and the geometry is not singular (the sectional curvatures scale as  $\alpha^0$ ). The scalar curvature, see eq. (4.30), is negative. The situation is similar to point 2 in the one qubit case.

So far we discussed complexity as defined for unitary operators. For applications to holography, it is more relevant to consider the different but somehow related notion of state complexity [8]. Complexity for states is defined as the lowest possible complexity of an operator which prepares the state, starting from a given reference state. In general, we have to minimise over all the possible unitaries that prepare the given state [52]. The complexity metric here is much more intricate, because the geometry is not homogeneous.

In section 5, we point out that the relation between the unitary and the state geometry follows directly from the mathematical theory of Riemannian submersions [53, 54, 63]. In particular, the geodesics in the state space  $B$  can be found by a projection of a particular class of geodesics (the horizontal ones) from the unitary space  $M$ . Moreover, conjugate points for geodesics in  $B$  are realised for a complexity equal or less than the one in  $M$ . Curvatures in the state and in the unitary spaces are related by O'Neill's formula [53]. Geodesics in the state space can be in principle computed without even knowing the metric on  $B$ . Our approach gives also a closed-form expression for the state metric.

We checked that this result reproduces the known 1-qubit metric with arbitrary penalties. As a new application, we determine the state complexity metric and curvatures for the qutrit example.

An important open problem is to understand the regime in which the complexity metric provides a complexity distance scaling exponentially with the number of qubits. In section 6 we provide robust evidence for the exponential behaviour of complexity for progressive penalties. The analysis is based on the study of conjugate points in the unitary space. For a general manifold, the study of conjugate points does not provide direct information about the maximal possible complexity, because a geodesic might cross its cut locus before the conjugate point. This obstruction can be circumvented if one considers parametric regimes in which the angular position of the conjugate point approaches the identity. In this limit we expect that the cut locus coincides with the conjugate point. We show that this regime is realised for progressive penalties at large  $\alpha$  and we give an estimate for a lower bound for the scaling of complexity. This bound scales exponentially with  $n$ .

## Acknowledgments

We are grateful to Mauro Spera for very precious geometrical insights. We thank Luca Cassia, Alice Gatti and Alessandro Tomasiello for valuable discussions.

S.B. acknowledges support from the Independent Research Fund Denmark grant number DFF-6108-00340 "Towards a deeper understanding of black holes with non-relativistic holography". A.L. is supported by UKRI Science and Technology Facilities Council (STFC) Consolidated Grants ST/P00055X/1 and ST/T000813/1. The work of G.B.D.L. is supported in part by the Simons Foundation Origins of the Universe Initiative (modern inflationary cosmology collaboration) and by a Simons Investigator award. N.Z. acknowledges the Ermenegildo Zegna's Group for the financial support.

## Appendix

### A Shear tensor equation

The Weyl tensor is given by

$$\begin{aligned} C_{\mu\alpha\nu\beta} &= -R_{\mu\alpha\nu\beta} + \frac{1}{d-2} (R_{\mu\beta}g_{\alpha\nu} - R_{\mu\nu}g_{\alpha\beta} + R_{\alpha\nu}g_{\mu\beta} - R_{\alpha\beta}g_{\mu\nu}) \\ &+ \frac{1}{(d-1)(d-2)} R (g_{\mu\nu}g_{\alpha\beta} - g_{\mu\beta}g_{\alpha\nu}) \end{aligned} \quad (\text{A.1})$$

and its contraction with the normalized velocity is

$$C_{\mu\alpha\nu\beta} u^\alpha(\sigma) u^\beta(\sigma) = \frac{1}{q_\sigma} C_{\mu\sigma\nu\sigma}. \quad (\text{A.2})$$

Recalling that in our basis  $R_{\mu\sigma\nu\sigma} = -R_{\mu\sigma\sigma\nu} \neq 0$  only if  $\mu = \nu$  and that both the metric and the Ricci tensor are diagonal, we conclude that  $C_{\mu\sigma\nu\sigma} \neq 0$  only if  $\mu = \nu$ . However, if  $\mu = \nu = \sigma$ , we have  $C_{\mu\sigma\nu\sigma} = 0$ . Therefore, the only relevant non-vanishing components of  $C_{\mu\sigma\nu\sigma}$  are the ones with  $\mu = \nu = \rho \neq \sigma$ . These components read

$$C_{\rho\sigma\rho\sigma} = q_\rho q_\sigma \left[ K(\rho, \sigma) - \frac{1}{d-2} (R_\rho + R_\sigma) + \frac{1}{(d-1)(d-2)} R \right]. \quad (\text{A.3})$$

The only non-vanishing components of the Weyl tensor contraction with the normalized velocity are the ones with  $\rho \neq \sigma$ :

$$C_{\rho\alpha\rho\beta} u^\alpha(\sigma) u^\beta(\sigma) = q_\rho \left[ K(\rho, \sigma) - \frac{1}{d-2} (R_\rho + R_\sigma) + \frac{1}{(d-1)(d-2)} R \right] \quad (\text{A.4})$$

A direct calculation gives that  $\bar{R}_{\mu\nu}$  is non-vanishing only if  $\mu = \nu = \rho \neq \sigma$ :

$$\bar{R}_{\rho\rho} = q_\rho \left[ \frac{R_{\rho\rho}}{q_\rho} - \frac{1}{d-1} (R - R_\sigma) \right] = q_\rho \left[ R_\rho - \frac{1}{d-1} (R - R_\sigma) \right]. \quad (\text{A.5})$$

The non-vanishing components of the tensor entering into the shear equation (6.6) are thus the ones with  $\rho \neq \sigma$ :

$$C_{\rho\alpha\rho\beta} u^\alpha(\sigma) u^\beta(\sigma) + \frac{1}{d-2} \bar{R}_{\rho\rho} = q_\rho \left\{ K(\rho, \sigma) - \frac{1}{d-1} R_\sigma \right\}. \quad (\text{A.6})$$

Note that in the 1-qubit case ( $d = 3$ ), by means of eqs. (3.1) and (6.17), all the components of the above tensor vanish for  $G_x$  if  $P = Q$ , for  $G_y$  if  $P = 1$  and for  $G_z$  if  $Q = 1$ . In these cases, from eq. (6.6) we get that if  $\sigma_{\alpha\beta} = 0$  it vanishes along all the geodesic.

## References

- [1] M. A. Nielsen, “A geometric approach to quantum circuit lower bounds”, [arXiv:0502070 [quantum-ph]].
- [2] M. A. Nielsen, M. Dowling, M. Gu and A. C. Doherty, “Quantum computation as geometry”, Science 311, 1133 (2006).
- [3] M. A. Nielsen, M. Dowling, M. Gu and A. C. Doherty, “Optimal control, geometry, and quantum computing”, Phys. Rev. A 73, 062323 (2006)
- [4] M. Gu, A. C. Doherty and M. A. Nielsen, “Quantum control via geometry: An explicit example”, Phys. Rev. A 78, 032337 (2008)
- [5] Mark R. Dowling, Michael A. Nielsen, “The geometry of quantum computation,” Quantum information and computation 8(10):861-899 January 2010, [arXiv:quant-ph/0701004](#)
- [6] L. Susskind, [Fortsch. Phys. **64** (2016) 24] Addendum: Fortsch. Phys. **64** (2016) 44 doi:10.1002/prop.201500093, 10.1002/prop.201500092 [[arXiv:1403.5695](#) [hep-th], [arXiv:1402.5674](#) [hep-th]].
- [7] D. Stanford and L. Susskind, Phys. Rev. D **90** (2014) no.12, 126007 doi:10.1103/PhysRevD.90.126007 [[arXiv:1406.2678](#) [hep-th]].
- [8] L. Susskind, Fortsch. Phys. **64** (2016) 49 doi:10.1002/prop.201500095 [[arXiv:1411.0690](#) [hep-th]].
- [9] L. Susskind, Fortsch. Phys. **64** (2016), 84-91 doi:10.1002/prop.201500091 [[arXiv:1507.02287](#) [hep-th]].
- [10] L. Susskind, [arXiv:1810.11563](#) [hep-th].
- [11] S. Ryu and T. Takayanagi, Phys. Rev. Lett. **96** (2006) 181602 doi:10.1103/PhysRevLett.96.181602 [[hep-th/0603001](#)].

- [12] D. N. Page, Phys. Rev. Lett. **71** (1993), 3743-3746 doi:10.1103/PhysRevLett.71.3743 [[arXiv:hep-th/9306083](#) [hep-th]].
- [13] A. Almheiri, N. Engelhardt, D. Marolf and H. Maxfield, JHEP **12** (2019), 063 doi:10.1007/JHEP12(2019)063 [[arXiv:1905.08762](#) [hep-th]].
- [14] G. Penington, JHEP **09** (2020), 002 doi:10.1007/JHEP09(2020)002 [[arXiv:1905.08255](#) [hep-th]].
- [15] A. Almheiri, R. Mahajan, J. Maldacena and Y. Zhao, JHEP **03** (2020), 149 doi:10.1007/JHEP03(2020)149 [[arXiv:1908.10996](#) [hep-th]].
- [16] A. R. Brown, D. A. Roberts, L. Susskind, B. Swingle and Y. Zhao, Phys. Rev. Lett. **116** (2016) no.19, 191301 doi:10.1103/PhysRevLett.116.191301 [[arXiv:1509.07876](#) [hep-th]].
- [17] A. R. Brown, D. A. Roberts, L. Susskind, B. Swingle and Y. Zhao, Phys. Rev. D **93** (2016) no.8, 086006 doi:10.1103/PhysRevD.93.086006 [[arXiv:1512.04993](#) [hep-th]].
- [18] L. Lehner, R. C. Myers, E. Poisson and R. D. Sorkin, Phys. Rev. D **94** (2016) no.8, 084046 doi:10.1103/PhysRevD.94.084046 [[arXiv:1609.00207](#) [hep-th]].
- [19] R. G. Cai, S. M. Ruan, S. J. Wang, R. Q. Yang and R. H. Peng, JHEP **1609** (2016) 161 doi:10.1007/JHEP09(2016)161 [[arXiv:1606.08307](#) [gr-qc]].
- [20] S. Chapman, H. Marrochio and R. C. Myers, JHEP **1701** (2017) 062 doi:10.1007/JHEP01(2017)062 [[arXiv:1610.08063](#) [hep-th]].
- [21] D. Carmi, S. Chapman, H. Marrochio, R. C. Myers and S. Sugishita, JHEP **1711** (2017) 188 doi:10.1007/JHEP11(2017)188 [[arXiv:1709.10184](#) [hep-th]].
- [22] P. Braccia, A. L. Cotrone and E. Tonni, JHEP **02** (2020), 051 doi:10.1007/JHEP02(2020)051 [[arXiv:1910.03489](#) [hep-th]].
- [23] J. L. F. Barbon and E. Rabinovici, JHEP **1601** (2016) 084 doi:10.1007/JHEP01(2016)084 [[arXiv:1509.09291](#) [hep-th]].
- [24] R. Auzzi, S. Baiguera and G. Nardelli, JHEP **1806** (2018) 063 doi:10.1007/JHEP06(2018)063 [[arXiv:1804.07521](#) [hep-th]].
- [25] R. Auzzi, S. Baiguera, M. Grassi, G. Nardelli and N. Zenoni, JHEP **1809** (2018) 013 doi:10.1007/JHEP09(2018)013 [[arXiv:1806.06216](#) [hep-th]].
- [26] M. Alishahiha, Phys. Rev. D **92** (2015) no.12, 126009 doi:10.1103/PhysRevD.92.126009 [[arXiv:1509.06614](#) [hep-th]].
- [27] D. Carmi, R. C. Myers and P. Rath, JHEP **1703** (2017) 118 doi:10.1007/JHEP03(2017)118 [[arXiv:1612.00433](#) [hep-th]].
- [28] O. Ben-Ami and D. Carmi, JHEP **1611** (2016) 129 doi:10.1007/JHEP11(2016)129 [[arXiv:1609.02514](#) [hep-th]].
- [29] R. Abt, J. Erdmenger, H. Hinrichsen, C. M. Melby-Thompson, R. Meyer, C. Northe and I. A. Reyes, Fortsch. Phys. **66** (2018) no.6, 1800034 doi:10.1002/prop.201800034 [[arXiv:1710.01327](#) [hep-th]].
- [30] C. A. Agón, M. Headrick and B. Swingle, JHEP **1902** (2019) 145 doi:10.1007/JHEP02(2019)145 [[arXiv:1804.01561](#) [hep-th]].

- [31] M. Alishahiha, K. Babaei Velni and M. R. Mohammadi Mozaffar, Phys. Rev. D **99** (2019) no.12, 126016 doi:10.1103/PhysRevD.99.126016 [[arXiv:1809.06031](#) [hep-th]].
- [32] E. Caceres, J. Couch, S. Eccles and W. Fischler, Phys. Rev. D **99** (2019) no.8, 086016 doi:10.1103/PhysRevD.99.086016 [[arXiv:1811.10650](#) [hep-th]].
- [33] R. Auzzi, S. Baiguera, A. Mitra, G. Nardelli and N. Zenoni, JHEP **09** (2019), 114 doi:10.1007/JHEP09(2019)114 [[arXiv:1906.09345](#) [hep-th]].
- [34] B. Chen, W. M. Li, R. Q. Yang, C. Y. Zhang and S. J. Zhang, JHEP **1807** (2018) 034 doi:10.1007/JHEP07(2018)034 [[arXiv:1803.06680](#) [hep-th]].
- [35] R. Auzzi, G. Nardelli, F. I. Schaposnik Massolo, G. Tallarita and N. Zenoni, JHEP **11** (2019), 098 doi:10.1007/JHEP11(2019)098 [[arXiv:1908.10832](#) [hep-th]].
- [36] R. Auzzi, S. Baiguera, A. Legramandi, G. Nardelli, P. Roy and N. Zenoni, JHEP **01** (2020), 066 doi:10.1007/JHEP01(2020)066 [[arXiv:1910.00526](#) [hep-th]].
- [37] E. Caceres, S. Chapman, J. D. Couch, J. P. Hernandez, R. C. Myers and S. M. Ruan, JHEP **03** (2020), 012 doi:10.1007/JHEP03(2020)012 [[arXiv:1909.10557](#) [hep-th]].
- [38] J. Hernandez, R. C. Myers and S. M. Ruan, [[arXiv:2010.16398](#) [hep-th]].
- [39] G. Di Giulio and E. Tonni, [[arXiv:2006.00921](#) [hep-th]].
- [40] R. Jefferson and R. C. Myers, JHEP **1710** (2017) 107 doi:10.1007/JHEP10(2017)107 [[arXiv:1707.08570](#) [hep-th]].
- [41] K. Hashimoto, N. Iizuka and S. Sugishita, Phys. Rev. D **96** (2017) no.12, 126001 doi:10.1103/PhysRevD.96.126001 [[arXiv:1707.03840](#) [hep-th]].
- [42] H. A. Camargo, P. Caputa, D. Das, M. P. Heller and R. Jefferson, Phys. Rev. Lett. **122** (2019) no.8, 081601 doi:10.1103/PhysRevLett.122.081601 [[arXiv:1807.07075](#) [hep-th]].
- [43] P. Caputa and J. M. Magan, Phys. Rev. Lett. **122** (2019) no.23, 231302 doi:10.1103/PhysRevLett.122.231302 [[arXiv:1807.04422](#) [hep-th]].
- [44] S. Chapman, J. Eisert, L. Hackl, M. P. Heller, R. Jefferson, H. Marrochio and R. C. Myers, SciPost Phys. **6** (2019) no.3, 034 doi:10.21468/SciPostPhys.6.3.034 [[arXiv:1810.05151](#) [hep-th]].
- [45] V. Balasubramanian, M. Decross, A. Kar and O. Parrikar, “Quantum Complexity of Time Evolution with Chaotic Hamiltonians,” JHEP **01** (2020), 134 doi:10.1007/JHEP01(2020)134 [[arXiv:1905.05765](#) [hep-th]].
- [46] A. R. Brown, L. Susskind and Y. Zhao, Phys. Rev. D **95** (2017) no.4, 045010 doi:10.1103/PhysRevD.95.045010 [[arXiv:1608.02612](#) [hep-th]].
- [47] A. R. Brown and L. Susskind, “Second law of quantum complexity,” Phys. Rev. D **97** (2018) no.8, 086015 doi:10.1103/PhysRevD.97.086015 [[arXiv:1701.01107](#) [hep-th]].
- [48] A. Bernamonti, F. Galli, J. Hernandez, R. C. Myers, S. M. Ruan and J. Simón, Phys. Rev. Lett. **123** (2019) no.8, 081601 doi:10.1103/PhysRevLett.123.081601 [[arXiv:1903.04511](#) [hep-th]].
- [49] A. Bernamonti, F. Galli, J. Hernandez, R. C. Myers, S. M. Ruan and J. Simón, doi:10.1088/1751-8121/ab8e66 [[arXiv:2002.05779](#) [hep-th]].

- [50] L. Susskind and Y. Zhao, [[arXiv:1408.2823](#) [hep-th]].
- [51] D. V. Anosov, “Geodesic flows on closed Riemann manifolds with negative curvature”, American Mathematical Society, Providence, R.I., 1969. MR 39 3527
- [52] A. R. Brown and L. Susskind, “Complexity geometry of a single qubit”, Phys. Rev. D **100** (2019) no.4, 046020 doi:10.1103/PhysRevD.100.046020 [[arXiv:1903.12621](#) [hep-th]].
- [53] B. O’Neill, “The fundamental equations of a submersion”, Michigan Math. J., Volume 13, Issue 4 (1966), 459-469.
- [54] B. O’Neill, “Submersions and geodesics”, Duke Math. J. Volume 34, Number 2 (1967), 363-373.
- [55] J. Milnor, “Curvatures of Left Invariant Metrics on Lie Groups,” Adv. Math. **21** (1976), 293-329 doi:10.1016/S0001-8708(76)80002-3
- [56] V. I. Arnold, “Mathematical Methods of Classical Mechanics,” Springer Verlag
- [57] Petersen, P., “Riemannian Geometry”
- [58] J. M. Lee, “Riemannian Manifolds - an introduction to curvature,” Springer
- [59] Keith Burns and Marlies Gerber, “Real analytic Bernoulli geodesic flows on  $S^2$ ”, Ergodic Theory Dynam. Systems 9 (1989), no. 1, 27-45. MR 991488, <https://doi.org/10.1017/S0143385700004806>
- [60] R. J. Caginalp and S. Leutheusser, [[arXiv:2010.15099](#) [hep-th]].
- [61] M. A. Nielsen, I. L. Chuang, “Quantum Computation and Quantum Information”, Cambridge University Press
- [62] L. Susskind, [[arXiv:2006.01280](#) [hep-th]].
- [63] A. L. Besse, “Einstein manifolds,” Springer
- [64] E. Poisson, “A Relativist’s Toolkit: The Mathematics of Black-Hole Mechanics,” doi:10.1017/CBO9780511606601
- [65] S. M. Carroll, “Spacetime and Geometry,”